ERR agonism reverses mitochondrial dysfunction and inflammation in the aging kidney

Xiaoxin X. Wang[1], Shogo Takahashi[1], Andrew E. Libby[1], Komuraiah Myakala[1], Bryce A. Jones[1], Kanchan Bhasin[1], Yue Qi[2], Kristopher Krausz[3], Patricia Zerfas[4], Julia Panov[5], Thomas J. Velenosi[3], Daxesh P. Patel[3], Parnaz Daneshpajouhnejad[6], Brandon Ginley[7], Pinaki Sarder[7], Avi Titievsky[5], Vadim Sharov[5], Boris Ostretsov[5], Jeffrey B Kopp[4], Avi Z Rosenberg[6], Frank J Gonzalez[3], Udayan Guha[2], Leonid Brodsky[5], Thomas Burris[8], Moshe Levi[1]

[1]Department of Biochemistry and Molecular and Cellular Biology, Georgetown University, Washington DC 20057, USA; [2]Thoracic and GI Malignancies Branch, National Cancer Institute, National Institutes of Health, Bethesda, MD 20814, USA; [3]Laboratory of Metabolism, Center for Cancer Research, National Cancer Institute, National Institutes of Health, Bethesda, MD 20892, USA; [4]Kidney Diseases Branch, National Institute of Diabetes and Digestive and Kidney Diseases, National Institutes of Health, Bethesda, MD 20814, USA; [5]Tauber Bioinformatics Research Center, University of Haifa, Mount Carmel, Haifa, 31905, Israel; [6]Department of Pathology, Johns Hopkins University School of Medicine, Renal Pathology Service, Baltimore, MD 21287, USA; [7]Departments of Pathology and Anatomical Sciences, Biostatistics, and Biomedical Engineering, University at Buffalo, The State University of New York, Buffalo, New York;[8]Center for Clinical Pharmacology, Washington University in St Louis, St. Louis, Missouri 63110, USA.

Correspondence:

Moshe Levi
Department of Biochemistry and Molecular & Cellular Biology,
Georgetown University,
3900 Reservoir Road, Basic Science 353,
Washington DC 20057, USA
Tel: 202-687-9296
E-mail: Moshe. Levi@georgetown.edu

ABSTRACT

A gradual decline in renal function occurs even in healthy aging individuals. In addition to aging per se, concurrent metabolic syndrome and hypertension, which are common in the aging population, can induce mitochondrial dysfunction, endoplasmic reticulum stress, oxidative stress, inflammation, altered lipid metabolism, and profibrotic growth factors in the kidney, which collectively contribute to age-related kidney disease. With increasing population of older individuals and the increasing incidence of acute kidney injury and chronic kidney disease, identifying preventable or treatable aspects of age-related nephropathy becomes of critical importance. In this regard we studied the role of the nuclear hormone receptors, the estrogen related receptors (ERRs), whose expression levels are decreased in aging human and mouse kidneys. Our studies have identified the estrogen related receptors ERRα, ERRβ, and ERRγ as important modulators of age-related mitochondrial dysfunction, cellular senescence, and inflammation. Significantly these pathways are also regulated by lifelong caloric restriction (CR), which is known to prevent several age-related complications including kidney disease. ERRα, ERRβ, and ERRγ expression levels are decreased in the aging kidney, and CR and pharmacological treatment with a pan ERR agonist results in increases in expression of ERRα, ERRβ, and ERRγ in the kidney. Remarkably, only a 4-week treatment of 21-month-old mice with the pan ERR agonist reversed the age-related mitochondrial dysfunction, the cellular senescence marker p21, and inflammatory cytokines, including the STAT3 and STING signaling pathways.

INTRODUCTION

The fastest growing group of people in the US with impaired kidney function is the 65 and older age group. This population is expected to double in the next 20 years, while the number worldwide is expected to triple from 743 million in 2009 to 2 billion in 2050. This will result in a marked increase in the elderly population with chronic kidney disease and acute kidney injury. This increase may be further amplified by other age-related co-morbidities including metabolic syndrome and hypertension that accelerate age-related decline in renal function [1-3]. Thus, there is increasing need for prevention and treatment strategies for age-related kidney disease.

A gradual decline in renal function occurs even in healthy aging individuals [4-6]. In addition to aging per se, metabolic syndrome and hypertension can induce mitochondrial dysfunction, endoplasmic reticulum stress, oxidative stress, inflammation, altered lipid metabolism, and profibrotic growth factors in the kidney, which collectively contribute to age-related kidney disease [4].

There is variation in the rate of decline in renal function as a function of gender, race, and burden of co-morbidities [7-10]. Greater glomerular, vascular and tubulointerstitial sclerosis is evident on renal tissue examination of healthy kidney donors with increasing age [11-13]. Interestingly, examination of processes leading to sclerosis suggests a role for possible modifiable systemic metabolic and hormonal factors that can ameliorate the rate of sclerosis. With the population of older individuals increasing, identifying preventable or treatable aspects of age-related nephropathy becomes of critical importance.

There is increasing evidence that mitochondrial biogenesis, mitochondrial function, mitochondrial unfolded protein response (UPR^{mt}), mitochondrial dynamics and mitophagy are impaired in aging, and these alterations result in several of the age-related diseases [14-21]. In this regard current research efforts are concentrated on modulating these molecular mechanisms to improve mitochondrial function.

Caloric restriction (CR) plays a prominent role in preventing age-related complications. We have previously shown that CR prevents age-related decline in renal function and renal lipid accumulation via inhibition of the sterol regulatory element binding proteins (SREBPs) [22, 23]. CR is also an important modulator of mitochondrial function. We have demonstrated that CR prevents age-related mitochondrial dysfunction in the kidney by increasing mitochondrial/nuclear DNA ratio, the mitochondrial transcription factor Nrf-1, AMPK, SIRT1, SIRT3, mitochondrial complex activities, mitochondrial IDH2, and mitochondrial fatty acid β-oxidation [24]. In addition, CR also prevents age-related decrease in mitochondrial abundance in the renal tubules. CR increases the renal expression of FXR and TGR5. Treatment of 22-month old mice fed ad lib (AL) for 2 months with the dual FXR-TGR5 agonist INT-767 reversed most of the age-related impairments in mitochondrial function and the progression of renal disease [24]. Importantly the FXR-TGR5 dual agonist as well as CR also increased expression of PGC-1α, ERRα and ERRγ, which are important regulators of mitochondrial biogenesis and function.

The estrogen-related receptors (ERR) ERRα (NR3B1, ESSRA gene), ERRβ (NR3B2, ESRRB gene), and ERRγ (NR3B3, ESRRG gene) are closely-related members of the nuclear receptor family. Except for one report [25], there are no known endogenous ligands for these orphan receptors. Importantly they do not bind natural estrogens, and they do not directly participate in classic estrogen signaling pathways or biological processes [26-28].

ERRα and ERRγ are strongly activated by their coactivators PGC-1α and PGC-1β [29, 30]. In contrast, RIP140 and NCoR1 are important corepressors of ERR activity [31, 32]. ERRs are also subject to post-translational modifications including phosphorylation, sumoylation, and acetylation that modulate the receptors' DNA binding and recruitment of coactivators [33-35].

ERRα and ERRγ regulate the transcription of genes involved in mitochondrial biogenesis, oxidative phosphorylation, tricarboxylic acid (TCA) cycle, fatty acid oxidation and glucose metabolism [28, 36-46]. However, in addition to overlapping gene activation there is also ample evidence that ERRα and ERRγ also have differential and opposing effects which can be due to interactions with corepressors, coactivators, posttranslational modification, or differential cell expression [28, 46]. Opposing effects for ERRα and ERRγ is seen in breast cancer [47, 48], regulation of gluconeogenesis in the liver [46, 47], skeletal muscle function [46, 47], macrophage function [46, 49, 50], and regulation of LDHA related to anaerobic glycolysis [28]. Finally, ERRα and ERRγ are highly expressed in the mouse and human kidney [51-53].

The roles of ERRα and ERRγ in modulating age-related impairment in mitochondrial function and age-related inflammation (inflammaging) are not known. We undertook our current studies to determine if a pan agonist of ERRs, including ERRα, ERRβ, and ERRγ, will improve mitochondrial dysfunction and inflammation in the aging kidney.

RESULTS

ERRα and ERRγ expression is decreased in the aging human kidney

In our previous study, we found that there is a decrease in the expression of ERRα and ERRγ in the aging kidney, and their expression is upregulated by the dual FXR-TGR5 agonist INT-767 treatment or caloric restriction, which correlated with increased mitochondrial biogenesis and function in the treated aging kidneys [24]. In view of the role of ERRs in mitochondrial biogenesis, we determined if this observed decreased expression also occurs in the human aging kidney. We performed immunohistochemistry with human kidney sections from young versus old individuals. The results indicate that both ERRα and ERRγ are expressed in renal tubules and their expression levels are markedly decreased in the aging human kidney samples (**Figure 1A**). Since ERRs are important modulators of mitochondrial biogenesis, we also stained the human kidney sections for the mitochondrial pyruvate dehydrogenase (PDH) e2/e3 and we found a marked decrease in PDH immunostaining in the aging human kidney samples (**Figure 1B**).

ERRα and ERRγ RNA distribution in the mouse kidney

To determine where ERRα and ERRγ are expressed in the kidney, we performed single nuclei RNAseq[54-57]. With 100k read depth and 3000-5000 nuclei sequenced, we were able to identify 12 clusters and assigned them to major cell types known in the mouse kidney (**Figure 2A**). We found most ERRα is expressed in proximal tubules, intercalated cells and podocytes. For ERRγ**,** we found proximal tubules and intercalated cells

express most of it. Compared to the young kidneys, aging proximal tubules at S1/S2 show decline in ERRα and ERRγ expression (**Figure 2B**).

Pan ERR agonist treatment increases the mRNA expression of *Errα, Errβ and Errγ* in the aging kidney

We found that *Errα, Errβ* and *Errγ* mRNA abundance is significantly decreased in the kidneys of aging mice. It should be noted however that *Errβ* expression level is at least 5-fold lower than either *Errα* or *Errγ* mRNA abundance. Treatment with the ERR pan agonist induces significant increases in the *Errα*, *Errβ* and *Errγ* mRNA abundance in the kidneys of aging mice, to levels observed in the young mice (**Figure 3**).

This prompted us to perform bulk RNAseq to determine which pathways are changed by the increased ERR activity. The data showed the main pathways upregulated by the treatment are mitochondrial related and the downregulated pathways are immune related (**Figure 4A**).

Proteomic analysis revealed that major pathways regulated included mitochondrial electron transport chain (ETC), tricarboxylic acid (TCA) cycle, and mitochondrial fatty acid β-oxidation (**Figure 4B**).

The multi-omics integration using O2PLS demonstrated a regulation pattern that separated old group from old with pan agonist group. They found pan agonist treatment

decreased pathways related to immune system activation in both gene expression and protein abundances (**Figure 4C**).

As the hallmarks for aging kidneys are decreased mitochondrial function and increased inflammation [58, 59], we then determined if treatment with the pan ERR agonist improved those defects in the aging kidneys.

Pan ERR agonist treatment restored mitochondrial function in aging kidneys

The canonical action of ERRs is to induce mitochondrial biogenesis. We have seen the increased expression in aging kidneys of master mitochondrial biogenesis regulator PGC1α/β and Tfam1 with pan ERR agonist treatment. As a result, mitochondrial DNA/nuclear DNA ratio is increased in the aging kidneys following treatment (**Figure 5**), an indicator of increased mitochondrial biogenesis.

ERR activation also increased the expression of genes related to mitochondrial electron transport chain (ETC) and tricarboxylic acid (TCA) cycle, such as complex I subunit *Ndufb8*, complex II subunit *Sdhc*, complex III subunit *Uqcrb*, complex IV subunit *Cox6a2*, complex V subunit *Atp5b* (**Figure 6A**), and *Pdhb*, *Mdh1*, *Idh3b*, and *Sucla2*, important enzymes for TCA cycle (**Figure 6B**). This is consistent with the increased succinic acid level, one of TCA intermediate metabolites, following the treatment (**Figure 6C**). The interrelationship between ETC and TCA cycle is illustrated in **Figure 6D**.

Mitochondrial ETC is also regulated by ERR agonism. Native blue gel showed the increased level of assembled complex II, III, IV and V after the treatment (**Figure 7A**). This results in the increased maximum respiration capacity in mitochondria isolated from aging kidneys (**Figure 7B**).

In addition, enzymes that mediate mitochondrial fatty acid β-oxidation including CPT-1a and MCAD mRNA is upregulated by the pan ERR agonist (**Figure 8**), suggesting the involvement of ERR agonism in promoting fatty acid oxidation.

Pan ERR agonist treatment altered mitochondrial dynamics in aging kidneys

Transmission electron microscopy showed alterations in the mitochondria of aging kidneys including decreases in the width and length of mitochondria, which were restored to levels seen in young kidneys upon treatment with the pan ERR agonist (**Figure 9A**).

Since these mitochondrial changes are reminiscent of alterations in mitochondrial fusion and fission, we also determined expression of proteins that regulate mitochondrial fusion and fission.

Opa1 protein localizes to the inner mitochondrial membrane and helps regulate mitochondrial stability, energy output, and mitochondrial fusion [60, 61]. While mRNA level was decreased, there was no significant change in the protein level in the aging kidney. However, upon treatment there was an increase in the mRNA level and a tendency for

the protein level to increase in the aging kidneys (**Figure 9B**). Mitofusin 2 is found in the outer membrane that surrounds mitochondria and participates in mitochondrial fusion [62]. There was a significant decrease in the aging kidney and the ERR pan agonist increased the protein abundance in both the young and the old kidneys, with the resulting levels in the old kidneys being the same as in the young kidneys (**Figure 9B**). In addition, there were also significant decreases in Mitoguardin 2 and MitoPLD mRNA levels in the aging kidneys that were normalized upon treatment with the pan ERR agonist (**Figure 9B**).

Drp1, is a member of the dynamin superfamily of proteins and is a fundamental component of mitochondrial fission [62-64]. We found that there were significant increases in Drp1 and phospho-Drp1 protein in the kidneys of aging mice, which were restored back to levels seen in young mice following treatment with the pan ERR agonist (**Figure 9C**).

Pan ERR agonist treatment decreased inflammation in aging kidneys

The cyclic GMP-AMP synthase (cGAS)-stimulator of interferon genes (STING) pathway has been reported to lead mitochondrial dysfunction to the activation of senescence and innate immune system [65, 66]. In the aging kidneys we found increased expression of STING mRNA and pan agonist can significantly lower its expression (**Figure 10A**). These changes are in parallel to the expression of senescence marker p21 which has been induced in the aging kidney and reduced by the treatment. Another marker p16 was found increased in the aging kidneys but no remarkable change after the treatment

(**Figure 10A**). Both markers have been found downregulated in the aging kidneys with life-long CR (**Figure 10B**). To find out which inflammatory factors are regulated by the pan agonist treatment we searched the RNAseq data and verified by the real-time PCR that the proinflammatory cytokine IL-1β and cell adhesion molecule ICAM1 were targeted by ERR agonist (**Figure 10C**). In addition, we observed the correspondent changes occurring to STAT3, a cytokine activated signaling pathway (**Figure 10D**). As a marker for STAT3 activation, we found a significant increase in p-Tyr705-STAT3 protein and total STAT3 protein that was decreased upon treatment with the pan ERR agonist.

DISCUSSION

Our studies have identified the nuclear hormone receptors the estrogen related receptors ERRα, ERRβ, and ERRγ as important modulators of age-related mitochondrial dysfunction, cellular senescence, and inflammation, that are also regulated by lifelong CR. ERRα, ERRβ, and ERRγ expression levels are decreased in the aging kidney, and caloric restriction results in increases in expression of ERRα, ERRβ, and ERRγ in the kidney.

Remarkably, only a 4-week treatment of 21-month-old mice with the pan ERR agonist reversed the age-related mitochondrial dysfunction, the cellular senescence marker p21, and inflammation. These effects were comparable with those achieved with lifelong CR, which is known to protect against age-related co-morbidities, including loss of renal function [22, 23, 67].

Recent evidence indicates that mitochondrial dysfunction of one of the mediators of cellular senescence and the associated senescence associated secretory phenotype (SASP) that includes pro-inflammatory cytokines and pro-fibrotic growth factors [68-74]. This process may also be involved in the age-related inflammation that has been termed inflammaging or senoinflammation, which is also prevented by CR [75-79].

Recently mitochondrial dysfunction has also been linked to activation of the cGMP-AMP synthase (cGAS)-stimulator of interferon genes (STING) signaling pathway, which plays key roles in immunity, inflammation, senescence and cancer [65, 66, 80-83]. In addition to the recent identification of the importance of this signaling pathway in mouse models of

chronic kidney disease and fibrosis [66], our studies also determine increased expression of STING in the aging kidneys, and its downregulation following treatment with the pan ERR agonist.

In addition to cGAS-STING signaling mitochondrial dysfunction is also associated with activation of STAT3 [84]. Increased STAT3 signaling is associated with senescence [85, 86] as well as kidney disease [87, 88]. We have found increased STAT in the aging kidneys both at the mRNA and protein level, including increased phospho-STAT3 (Tyr^{705}) and normalization after treatment with the pan ERR agonist.

At this time, it is not known whether the ERR induced decreases in STAT3 and STING mediate the decrease in the senescent cell marker p21 followed by decreases in IL-1β and ICAM1. However, our studies identify the ERRs as modulators of mitochondrial function, senescence, and inflammation in the aging kidney.

METHODS

Mice: Studies were performed in 4-month-old and 21-month-old male C57BL/6 male mice obtained through the NIA aging rodent colony. The mice were treated with 3% DMSO or the pan ERR agonist SLU-PP-332 at 25 mg/kg body weight/day administered intraperitoneally. The mice were treated for 4 weeks, following week they underwent anesthesia and the kidneys were harvested and processed for a) histology, b) transmission electron microscopy, c) isolation of nuclei, d) isolation of mitochondria, and e) biochemical studies detailed below.

Immunohistochemistry: Formalin-fixed paraffin-embedded tissue sections were subjected to antigen retrieval with EDTA buffer in high pressure heated water bath and staining was performed using either mouse monoclonal ERRα (1:2500, Abcam, Cambridge, MA) or ERRγ (1:400, Abcam) antibodies for 90 minutes or pyruvate dehydrogenase E2/E3bp (1:1000, Abcam) antibody for 45 minutes. Then UnoVue HRP secondary antibody detection reagent (Diagnostic BioSystems, Pleasanton, CA) was applied followed by DAB chromogen. The imaging was taken with Nanozoomer (Hamamatsu Photonics, Japan).

Transmission Electron Microscopy: One mm^3 cortex kidney tissues were fixed for 48 hrs. at 4^oC in 2.5% glutaraldehyde and 1% paraformaldehyde in 0.1M cacodylate buffer (pH 7.4) and washed with cacodylate buffer three times. The tissues were fixed with 1% OsO_4 for two hours, washed again with 0.1M cacodylate buffer three times, washed with

water and placed in 1% uranyl acetate for one hour. The tissues were subsequently serially dehydrated in ethanol and propylene oxide and embedded in EMBed 812 resin (Electron Microscopy Sciences, Hatfield, PA, USA). Thin sections, approx. 80 nm, were obtained by utilizing the Leica ultracut-UCT ultramicrotome (Leica, Deerfield, IL) and placed onto 300 mesh copper grids and stained with saturated uranyl acetate in 50% methanol and then with lead citrate. The grids were viewed with a JEM-1200EXII electron microscope (JEOL Ltd, Tokyo, Japan) at 80kV and images were recorded on the XR611M, mid mounted, 10.5M pixel, CCD camera (Advanced Microscopy Techniques Corp, Danvers, MA).

The minimum diameter of the mitochondrial short axis was measured in a minimum of 6 TEM images from each mouse (n = 3-4 each group). All mitochondria that were completely within the image field were measured. For each group, the image with the median diameter of the mitochondrial short axis closest to the median diameter for the whole group was chosen as the representative image. If two images were equally close, the image with a more normal distribution was chosen as the representative image for the group.

RNA extraction and real-time quantitative PCR: Total RNA was isolated from the kidneys using Qiagen RNeasy mini kit (Valencia, CA), and cDNA was synthesized using reverse transcript reagents from Thermo Fisher Scientific (Waltham, MA). Quantitative real-time PCR was performed as previously described [89-92], and expression levels of

target genes were normalized to 18S level. Primer sequences are listed in **Supplementary Table 1**.

RNA-seq: Approximately 300-500ng of kidneys RNA were used to generate barcoded RNA libraries using Ion AmpliSeq™ Transcriptome Mouse Gene Expression Panel, Chef-Ready Kit. Precise library quantification was performed using the Ion Library Quantitation Kit (Thermo Fisher Scientific). Sequencing was performed on an Ion Proton with signal processing and base calling using Ion Torrent Suite (Thermo Fisher Scientific). Raw sequence was mapped to Ampliseq supported mm10 transcriptome. Quality control metrics and normalized read counts per million were generated using the RNA-seq Analysis plugin (Ion Torrent Community, Thermo Fisher Scientific).

RNA-seq of single nuclei: Mouse kidney single nuclei were isolated [54-57] and counted using the EVE Automated Cell Counter (NanoEnTek, VWR). The resulting mixture was provided to the Genomics and Epigenomics Shared Resource (GESR) at Georgetown University, and further processed by the Chromium Controller (10X Genomics, Pleasanton, CA) using Single Cell 3' GEM Kit v3, Single Cell 3' Library Kit v3, i7 multiplex kit, Single Cell 3' Gel Bead Kit v3 (10X Genomics) according to the manufacturer's instructions with modifications for single nuclei. Libraries were sequenced on the Illumina Novaseq S4 System (Illumina, San Diego, CA) to an average depth of >300 M reads PF per sample. Data Analysis: The 10XGenomics BCL data was loaded into the Cellranger Makefastq pipeline, which demultiplexes raw base call (BCL) files generated by Illumina sequencers into FASTQ files which are further analyzed by the Cellranger Count pipeline.

Inside the Cellranger Count pipeline, SART was used to align sequencing reads to Mouse MM10 genome reference. The Cloupe files were obtained and were further visually investigated by the Loupe Cell Browser.

Proteomics: Proteomics studies were conducted with Udayan Guha and Yue Qi at CCR, NCI, NIH. 200 microgram of cortical kidney sections were homogenized and lysed by 8M urea in 20mM HEPES (pH=8.0) buffer with protease and phosphatase inhibitors using Tissue Lyser II (QIAGEN). Samples were reduced and alkylated followed by MS-grade trypsin digestion. The resulting tryptic peptides were labeled with 11 plex tandem mass tag (TMT). After quench, the tagged peptides were combined and fractionated with basic-pH reverse-phase high-performance liquid chromatography, collected in a 96-well plate and combined for a total of 12 fractions prior to desalting and subsequent liquid chromatography−tandem mass spectrometry (LC−MS/MS) processing on a Orbitrap Q-Exactive HF (Thermo Fisher Scientific) mass spectrometer interfaced with an Ultimate 3000 nanoflow LC system [93]. Each fraction was separated on a reverse phase C_{18} nano-column (25μm × 75cm, 2μm particles) with a linear gradient 4~45% solvent B (0.1% TFA in Acetonitrile). Data dependent mode was applied to analyze the top 15 most abundant peaks in one acquisition cycle.

MS raw files were mapped against Uniprot mouse database (version 20170207) using the MaxQuant software package (version 1.5.3.30) with the Andromeda search engine [94, 95]. Corrected intensities of the reporter ions from TMT labels were obtained from the MaxQuant search. For the TMT experiment, relative ratios of each channel to the

reference channel (channel11, pooled from 20 samples) were calculated. Perseus (version 1.5.5.3) was used to further analyze and visualize the data. Hierarchical clustering of proteins was obtained in Perseus using log ratios or log intensities of protein abundance.

Metabolomic and Lipidomics analysis: These studies were conducted with Dr. Frank J. Gonzalez, Shogo Takahashi and Thomas J. Velenosi, and Daxesh P. Patel, CCR, National Cancer Institute, NIH. In these studies, we determined metabolites and lipid profiles in kidneys using Q-TOF-MS [96-101]. Samples were analyzed by HILIC (Hydrophilic-interaction-liquid-chromatography) separation and mass spectrometry using a Waters Acquity H-class UPLC coupled to a Xevo G2 Q-Tof mass spectrometer for metabolomics. For lipidomics, samples were analyzed by UPLC-ESI-QTOFMS using a Waters Acquity CSH 1.7 µm C18 column (2.1x100 mm) (92, 93). For metabolomic and lipidomic data analysis, centroided and integrated chromatographic mass data was processed by Progenesis QI (Waters Corp., Milford, MA) to generate a multivariate data matrix. MS-DIAL (http://prime.psc.riken.jp/Metabolomics_Software/MS-DIAL/) and MS-FINDER (http://prime.psc.riken.jp/Metabolomics_Software/MS-FINDER/index.html) software was used for metabolites and lipid annotation [102, 103]. The matrices were analyzed by principal components analysis (PCA) and supervised orthogonal projection to latent structures (OPLS) analysis using SIMCA. The OPLS, loadings scatter and S-plot analysis by SIMCA software were used to determine those ions that contribute to separation between groups.

Mitochondrial isolation: Kidney mitochondria were isolated using the kit from Sigma (St. Louis, MO) and followed the instruction accordingly.

Mitochondrial Biogenesis: We measured mitochondrial and nuclear DNA by RT-QPCR.

Mitochondrial Respiration: We measured basal respiration, ATP turnover, proton leak, maximal respiration and spare respiratory capacity using the *Seahorse* XF96 Analyzer on equally loaded freshly isolated mitochondria. We also measured mitochondrial complex I, II, III, IV, and V protein abundance by Native Blue Gel Electrophoresis (Thermo Fisher Scientific) with equally loaded mitochondrial fractions.

Multi-omics data analysis and integration bioinformatics methods: The project includes several types of omics data (proteomics, transcriptomics, metabolomics, and lipidomics) measured in the same set of biological samples. Taking the advantage of this multi-omics set of measurements that reflects the same biological processes in the samples from different perspectives, we performed Two-way Orthogonal Partial Least Square (O2PLS) integration [104] in pairs of the transcriptomics, proteomics, metabolomics, and lipidomics datasets. As result of each omics pair integration, matching orthogonal components in dataset-members of the pair were found that show what major mutually coordinated regulations were found in this particular pair of the omics datasets.

Majority of the gene expression and protein abundance profiles can be presented as combinations in different proportions of these three o2PLS components. An association of a gene/protein profile with one of individual components is defined by “loading” of the profile on this particular component – how high is a projection of the profile as a vector of the sample-values on the component as also a vector of the sample values. Subsets of the most associated with individual components genes and proteins were determined.

Western blotting: Western blotting was performed as previously described [89-92]. Equal amount of total protein was separated by SDS-PAGE gels and transferred onto PVDF membranes. After HRP-conjugated secondary antibodies, the immune complexes were detected by chemiluminescence captured on Azure C300 digital imager (Dublin, CA) and the densitometry was performed with ImageJ software. Primary antibodies used for western blotting were listed in **Supplementary Table 1**.

FIGURE LEGENDS

Figure 1. ERRα, ERRγ, and PDH expression is decreased in the aging human kidney. **A)** ERRα and ERRγ immunohistochemistry on kidney sections from young and old subjects. The nuclear positive staining for ERRα or ERRγ is decreased in old kidney sections. **B)** PDH immunohistochemistry on kidney sections from young and old subjects. PDH staining is decreased in old kidney sections.

Figure 2. Single nuclei RNAseq of young and old kidneys. **A)** With 100k read depth and 3000-5000 nuclei sequenced, we were able to identify 12 clusters and assigned them to major cell types known in the mouse kidney. **B**) We found most ERRα is expressed in proximal tubules, intercalated cells and podocytes. For ERRγ**,** we found proximal tubules and intercalated cells express most of it. Compared to the young kidneys, aging proximal tubules at S1/S2 show decline in ERRα and ERRγ expression.

Figure 3. ERRα, ERRβ and ERRγ mRNA expression are decreased in the cortex of aging mouse kidneys. Treatment with the pan ERR agonist restores the mRNA levels of ERRα, ERRβ and ERRγ to levels seen in young kidneys.

Figure 4. RNAseq and proteomics of kidney cortex from old mice treated with vehicle or the pan ERR agonist. **A)** Pan ERR agonist increases expression of genes related to metabolism, TCA cycle, oxidative phosphorylation and ETC, while it decreases expression of genes related to inflammation, cytokine signaling, and innate immune

system. **B)** Pan ERR agonist increases abundance of proteins related to metabolism, ETC, and fatty acid β-oxidation. **C)** The multi-omics integration using O2PLS demonstrated a regulation pattern that separated old group from old with pan ERR agonist treatment group. Pan ERR agonist treatment decreased pathways related to immune system activation in both gene expression and protein abundances.

Figure 5. Pan ERR agonist treatment in old mice increases the expression of PCG1α and PGC1β, coregulators of ERRs and mediators of mitochondrial biogenesis. The expression of the mitochondrial transcription factor Tfam1 is decreased in the kidneys of old mice and pan ERR agonist treatment restores it to levels seen in young mice. Mitochondria to nuclear DNA ratio is decreased in the kidneys of old mice and pan ERR agonist treatment restores it to levels seen in young mice, indicative of increased mitochondrial biogenesis.

Figure 6. A) Mitochondrial ETC complex I-V marker expression is decreased in the kidneys of old mice and pan ERR agonist treatment restores it to levels seen in young mice, indicative of improvement in ETC. **B)** mRNA expression levels of the TCA cycle intermediates are decreased in the kidneys of old mice and pan ERR agonist treatment restores it to levels seen in young mice, indicative of restoration of the TCA cycle. **C)** Succinic acid levels are increased in the kidneys of old mice treated with the pan ERR agonist. **D)** Interrelationship of the TCA cycle and ETC.

Figure 7. A) Native blue gel indicates the increased level of assembled complex II, III, IV and V in the kidneys of old mice after treatment with the pan ERR agonist. **B)** Maximum respiration capacity in mitochondria isolated from the kidneys shows a significant impairment in old mice, which is restored to levels seen in young mice after treatment with the pan ERR agonist.

Figure 8. The fatty acid β-oxidation enzymes Cpt1a and MCAD mRNA levels are decreased in the kidneys of old mice, which are restored to levels seen in young mice after treatment with the pan ERR agonist.

Figure 9. A) Transmission electron microscopy showed alterations in the mitochondria of aging kidneys including decreases in the width and length of mitochondria, which were restored to levels seen in young kidneys upon treatment with the pan ERR agonist. **B)** There was a significant decrease in Mitofusin 2 protein abundance in the old kidneys and the ERR pan agonist increased the protein abundance in both the young and the old kidneys, with the resulting levels in the old kidneys being the same as in the young kidneys. In contrast, there was no significant change in the protein level of Opa1 in the old kidneys. However, upon treatment with the pan ERR agonist, there was a tendency for the protein level to increase in the aging kidneys. In addition, there were also significant decreases in Mitoguardin 2 and MitoPLD mRNA levels in the aging kidneys that were normalized upon treatment with the pan ERR agonist. **C)** There were significant increases in Drp1 and phospho-Drp1 protein in the kidneys of old mice,

which were restored back to levels seen in young mice following treatment with the pan ERR agonist.

Figure 10. A) There are significant increases in STING, p21 and p16 mRNA in the kidneys of old mice. Treatment with the pan ERR agonist decreases expression of STING and p21 but not p16 in the kidneys of old mice. **B)** Life-long caloric restriction (CR) prevents the increases in p21 and p16 in the kidneys of old mice. **C)** There are significant increases in the proinflammatory cytokine IL-1β and ICAM1 mRNA in the kidneys of old mice and treatment with the pan ERR agonist decreases their expression. **D)** There are significant increases in STAT3 mRNA and p-Tyr705-STAT3 protein in the kidneys of old mice and treatment with the pan ERR agonist decreases their expression to levels seen in the kidneys of young mice.

ACKNOWLEDGEMENTS

The above study is supported by NIA R01 AG049493 and NIDDK R01 DK116567 to M.L. and AHA postdoctoral fellowship to K.M. (19POST34381041) and A.E. L. (19POST34430001).

REFERENCES

1. Tonelli, M, Riella, M: Chronic kidney disease and the aging population. *American journal of physiology Renal physiology,* 306**:** F469-472, 2014.
2. Glassock, RJ, Rule, AD: The implications of anatomical and functional changes of the aging kidney: with an emphasis on the glomeruli. *Kidney international,* 82**:** 270-277, 2012.
3. Musso, CG, Oreopoulos, DG: Aging and physiological changes of the kidneys including changes in glomerular filtration rate. *Nephron Physiology,* 119 Suppl 1**:** p1-5, 2011.
4. Choudhury, D, Levi, M: Kidney aging--inevitable or preventable? *Nature reviews Nephrology,* 7**:** 706-717, 2011.
5. Bitzer, M, Wiggins, J: Aging Biology in the Kidney. *Advances in chronic kidney disease,* 23**:** 12-18, 2016.
6. Hodgin, JB, Bitzer, M, Wickman, L, Afshinnia, F, Wang, SQ, O'Connor, C, Yang, Y, Meadowbrooke, C, Chowdhury, M, Kikuchi, M, Wiggins, JE, Wiggins, RC: Glomerular Aging and Focal Global Glomerulosclerosis: A Podometric Perspective. *Journal of the American Society of Nephrology : JASN,* 26**:** 3162-3178, 2015.
7. Berg, UB: Differences in decline in GFR with age between males and females. Reference data on clearances of inulin and PAH in potential kidney donors. *Nephrology, dialysis, transplantation : official publication of the European Dialysis and Transplant Association - European Renal Association,* 21**:** 2577-2582, 2006.
8. Tauchi, H, Tsuboi, K, Okutomi, J: Age changes in the human kidney of the different races. *Gerontologia,* 17**:** 87-97, 1971.
9. Fliser, D, Franek, E, Joest, M, Block, S, Mutschler, E, Ritz, E: Renal function in the elderly: impact of hypertension and cardiac function. *Kidney international,* 51**:** 1196-1204, 1997.
10. Ribstein, J, Du Cailar, G, Mimran, A: Glucose tolerance and age-associated decline in renal function of hypertensive patients. *J Hypertens,* 19**:** 2257-2264, 2001.
11. Rule, AD, Amer, H, Cornell, LD, Taler, SJ, Cosio, FG, Kremers, WK, Textor, SC, Stegall, MD: The association between age and nephrosclerosis on renal biopsy among healthy adults. *Ann Intern Med,* 152**:** 561-567, 2010.
12. Hommos, MS, Zeng, C, Liu, Z, Troost, JP, Rosenberg, AZ, Palmer, M, Kremers, WK, Cornell, LD, Fervenza, FC, Barisoni, L, Rule, AD: Global glomerulosclerosis with nephrotic syndrome; the clinical importance of age adjustment. *Kidney international*, 2017.
13. Hommos, MS, Glassock, RJ, Rule, AD: Structural and Functional Changes in Human Kidneys with Healthy Aging. *Journal of the American Society of Nephrology : JASN,* 28**:** 2838-2844, 2017.
14. Madreiter-Sokolowski, CT, Sokolowski, AA, Waldeck-Weiermair, M, Malli, R, Graier, WF: Targeting Mitochondria to Counteract Age-Related Cellular Dysfunction. *Genes (Basel),* 9, 2018.
15. Jang, JY, Blum, A, Liu, J, Finkel, T: The role of mitochondria in aging. *J Clin Invest,* 128**:** 3662-3670, 2018.

16. Kauppila, TES, Kauppila, JHK, Larsson, NG: Mammalian Mitochondria and Aging: An Update. *Cell Metab,* 25**:** 57-71, 2017.
17. Lane, RK, Hilsabeck, T, Rea, SL: The role of mitochondrial dysfunction in age-related diseases. *Biochim Biophys Acta,* 1847**:** 1387-1400, 2015.
18. Fang, EF, Scheibye-Knudsen, M, Chua, KF, Mattson, MP, Croteau, DL, Bohr, VA: Nuclear DNA damage signalling to mitochondria in ageing. *Nat Rev Mol Cell Biol,* 17**:** 308-321, 2016.
19. Fakouri, NB, Hou, Y, Demarest, TG, Christiansen, LS, Okur, MN, Mohanty, JG, Croteau, DL, Bohr, VA: Toward understanding genomic instability, mitochondrial dysfunction and aging. *FEBS J*, 2018.
20. Shpilka, T, Haynes, CM: The mitochondrial UPR: mechanisms, physiological functions and implications in ageing. *Nat Rev Mol Cell Biol,* 19**:** 109-120, 2018.
21. Hansen, M, Rubinsztein, DC, Walker, DW: Autophagy as a promoter of longevity: insights from model organisms. *Nat Rev Mol Cell Biol,* 19**:** 579-593, 2018.
22. Jiang, T, Liebman, SE, Lucia, MS, Li, J, Levi, M: Role of altered renal lipid metabolism and the sterol regulatory element binding proteins in the pathogenesis of age-related renal disease. *Kidney Int,* 68**:** 2608-2620, 2005.
23. Jiang, T, Liebman, SE, Lucia, MS, Phillips, CL, Levi, M: Calorie restriction modulates renal expression of sterol regulatory element binding proteins, lipid accumulation, and age-related renal disease. *J Am Soc Nephrol,* 16**:** 2385-2394, 2005.
24. Wang, XX, Luo, Y, Wang, D, Adorini, L, Pruzanski, M, Dobrinskikh, E, Levi, M: A dual agonist of farnesoid X receptor (FXR) and the G protein-coupled receptor TGR5, INT-767, reverses age-related kidney disease in mice. *J Biol Chem,* 292**:** 12018-12024, 2017.
25. Wei, W, Schwaid, AG, Wang, X, Wang, X, Chen, S, Chu, Q, Saghatelian, A, Wan, Y: Ligand Activation of ERRalpha by Cholesterol Mediates Statin and Bisphosphonate Effects. *Cell Metab,* 23**:** 479-491, 2016.
26. Giguere, V, Yang, N, Segui, P, Evans, RM: Identification of a new class of steroid hormone receptors. *Nature,* 331**:** 91-94, 1988.
27. Giguere, V: Transcriptional control of energy homeostasis by the estrogen-related receptors. *Endocr Rev,* 29**:** 677-696, 2008.
28. Audet-Walsh, E, Giguere, V: The multiple universes of estrogen-related receptor alpha and gamma in metabolic control and related diseases. *Acta Pharmacol Sin,* 36**:** 51-61, 2015.
29. Finck, BN, Kelly, DP: PGC-1 coactivators: inducible regulators of energy metabolism in health and disease. *J Clin Invest,* 116**:** 615-622, 2006.
30. Lin, J, Handschin, C, Spiegelman, BM: Metabolic control through the PGC-1 family of transcription coactivators. *Cell Metab,* 1**:** 361-370, 2005.
31. Fritah, A, Christian, M, Parker, MG: The metabolic coregulator RIP140: an update. *Am J Physiol Endocrinol Metab,* 299**:** E335-340, 2010.
32. Yamamoto, H, Williams, EG, Mouchiroud, L, Canto, C, Fan, W, Downes, M, Heligon, C, Barish, GD, Desvergne, B, Evans, RM, Schoonjans, K, Auwerx, J: NCoR1 is a conserved physiological modulator of muscle mass and oxidative function. *Cell,* 147**:** 827-839, 2011.

33. Tremblay, AM, Wilson, BJ, Yang, XJ, Giguere, V: Phosphorylation-dependent sumoylation regulates estrogen-related receptor-alpha and -gamma transcriptional activity through a synergy control motif. *Mol Endocrinol,* 22**:** 570-584, 2008.
34. Vu, EH, Kraus, RJ, Mertz, JE: Phosphorylation-dependent sumoylation of estrogen-related receptor alpha1. *Biochemistry,* 46**:** 9795-9804, 2007.
35. Wilson, BJ, Tremblay, AM, Deblois, G, Sylvain-Drolet, G, Giguere, V: An acetylation switch modulates the transcriptional activity of estrogen-related receptor alpha. *Mol Endocrinol,* 24**:** 1349-1358, 2010.
36. Arany, Z, Foo, SY, Ma, Y, Ruas, JL, Bommi-Reddy, A, Girnun, G, Cooper, M, Laznik, D, Chinsomboon, J, Rangwala, SM, Baek, KH, Rosenzweig, A, Spiegelman, BM: HIF-independent regulation of VEGF and angiogenesis by the transcriptional coactivator PGC-1alpha. *Nature,* 451**:** 1008-1012, 2008.
37. Huss, JM, Torra, IP, Staels, B, Giguere, V, Kelly, DP: Estrogen-related receptor alpha directs peroxisome proliferator-activated receptor alpha signaling in the transcriptional control of energy metabolism in cardiac and skeletal muscle. *Mol Cell Biol,* 24**:** 9079-9091, 2004.
38. Mootha, VK, Handschin, C, Arlow, D, Xie, X, St Pierre, J, Sihag, S, Yang, W, Altshuler, D, Puigserver, P, Patterson, N, Willy, PJ, Schulman, IG, Heyman, RA, Lander, ES, Spiegelman, BM: Erralpha and Gabpa/b specify PGC-1alpha-dependent oxidative phosphorylation gene expression that is altered in diabetic muscle. *Proc Natl Acad Sci U S A,* 101**:** 6570-6575, 2004.
39. Schreiber, SN, Emter, R, Hock, MB, Knutti, D, Cardenas, J, Podvinec, M, Oakeley, EJ, Kralli, A: The estrogen-related receptor alpha (ERRalpha) functions in PPARgamma coactivator 1alpha (PGC-1alpha)-induced mitochondrial biogenesis. *Proc Natl Acad Sci U S A,* 101**:** 6472-6477, 2004.
40. Dixen, K, Basse, AL, Murholm, M, Isidor, MS, Hansen, LH, Petersen, MC, Madsen, L, Petrovic, N, Nedergaard, J, Quistorff, B, Hansen, JB: ERRgamma enhances UCP1 expression and fatty acid oxidation in brown adipocytes. *Obesity (Silver Spring),* 21**:** 516-524, 2013.
41. Dufour, CR, Wilson, BJ, Huss, JM, Kelly, DP, Alaynick, WA, Downes, M, Evans, RM, Blanchette, M, Giguere, V: Genome-wide orchestration of cardiac functions by the orphan nuclear receptors ERRalpha and gamma. *Cell Metab,* 5**:** 345-356, 2007.
42. Eichner, LJ, Giguere, V: Estrogen related receptors (ERRs): a new dawn in transcriptional control of mitochondrial gene networks. *Mitochondrion,* 11**:** 544-552, 2011.
43. Hock, MB, Kralli, A: Transcriptional control of mitochondrial biogenesis and function. *Annu Rev Physiol,* 71**:** 177-203, 2009.
44. Gantner, ML, Hazen, BC, Conkright, J, Kralli, A: GADD45gamma regulates the thermogenic capacity of brown adipose tissue. *Proc Natl Acad Sci U S A,* 111**:** 11870-11875, 2014.
45. Deblois, G, Giguere, V: Functional and physiological genomics of estrogen-related receptors (ERRs) in health and disease. *Biochim Biophys Acta,* 1812**:** 1032-1040, 2011.

46. Huss, JM, Garbacz, WG, Xie, W: Constitutive activities of estrogen-related receptors: Transcriptional regulation of metabolism by the ERR pathways in health and disease. *Biochim Biophys Acta,* 1852**:** 1912-1927, 2015.
47. Ariazi, EA, Clark, GM, Mertz, JE: Estrogen-related receptor alpha and estrogen-related receptor gamma associate with unfavorable and favorable biomarkers, respectively, in human breast cancer. *Cancer Res,* 62**:** 6510-6518, 2002.
48. Misawa, A, Inoue, S: Estrogen-Related Receptors in Breast Cancer and Prostate Cancer. *Front Endocrinol (Lausanne),* 6**:** 83, 2015.
49. Sonoda, J, Laganiere, J, Mehl, IR, Barish, GD, Chong, LW, Li, X, Scheffler, IE, Mock, DC, Bataille, AR, Robert, F, Lee, CH, Giguere, V, Evans, RM: Nuclear receptor ERR alpha and coactivator PGC-1 beta are effectors of IFN-gamma-induced host defense. *Genes Dev,* 21**:** 1909-1920, 2007.
50. Kim, DK, Jeong, JH, Lee, JM, Kim, KS, Park, SH, Kim, YD, Koh, M, Shin, M, Jung, YS, Kim, HS, Lee, TH, Oh, BC, Kim, JI, Park, HT, Jeong, WI, Lee, CH, Park, SB, Min, JJ, Jung, SI, Choi, SY, Choy, HE, Choi, HS: Inverse agonist of estrogen-related receptor gamma controls Salmonella typhimurium infection by modulating host iron homeostasis. *Nat Med,* 20**:** 419-424, 2014.
51. Bookout, AL, Jeong, Y, Downes, M, Yu, RT, Evans, RM, Mangelsdorf, DJ: Anatomical profiling of nuclear receptor expression reveals a hierarchical transcriptional network. *Cell,* 126**:** 789-799, 2006.
52. Berry, R, Harewood, L, Pei, L, Fisher, M, Brownstein, D, Ross, A, Alaynick, WA, Moss, J, Hastie, ND, Hohenstein, P, Davies, JA, Evans, RM, FitzPatrick, DR: Esrrg functions in early branch generation of the ureteric bud and is essential for normal development of the renal papilla. *Hum Mol Genet,* 20**:** 917-926, 2011.
53. Zhang, Z, Teng, CT: Interplay between estrogen-related receptor alpha (ERRalpha) and gamma (ERRgamma) on the regulation of ERRalpha gene expression. *Mol Cell Endocrinol,* 264**:** 128-141, 2007.
54. Park, J, Shrestha, R, Qiu, C, Kondo, A, Huang, S, Werth, M, Li, M, Barasch, J, Susztak, K: Single-cell transcriptomics of the mouse kidney reveals potential cellular targets of kidney disease. *Science,* 360**:** 758-763, 2018.
55. Wu, H, Kirita, Y, Donnelly, EL, Humphreys, BD: Advantages of Single-Nucleus over Single-Cell RNA Sequencing of Adult Kidney: Rare Cell Types and Novel Cell States Revealed in Fibrosis. *J Am Soc Nephrol,* 30**:** 23-32, 2019.
56. Wu, H, Malone, AF, Donnelly, EL, Kirita, Y, Uchimura, K, Ramakrishnan, SM, Gaut, JP, Humphreys, BD: Single-Cell Transcriptomics of a Human Kidney Allograft Biopsy Specimen Defines a Diverse Inflammatory Response. *J Am Soc Nephrol,* 29**:** 2069-2080, 2018.
57. Fu, J, Akat, KM, Sun, Z, Zhang, W, Schlondorff, D, Liu, Z, Tuschl, T, Lee, K, He, JC: Single-Cell RNA Profiling of Glomerular Cells Shows Dynamic Changes in Experimental Diabetic Kidney Disease. *J Am Soc Nephrol*, 2019.
58. Haas, RH: Mitochondrial Dysfunction in Aging and Diseases of Aging. *Biology (Basel),* 8, 2019.
59. Sato, Y, Yanagita, M: Immunology of the ageing kidney. *Nature Reviews Nephrology*, 2019.
60. Del Dotto, V, Mishra, P, Vidoni, S, Fogazza, M, Maresca, A, Caporali, L, McCaffery, JM, Cappelletti, M, Baruffini, E, Lenaers, G, Chan, D, Rugolo, M, Carelli, V,

Zanna, C: OPA1 Isoforms in the Hierarchical Organization of Mitochondrial Functions. *Cell Rep,* 19**:** 2557-2571, 2017.
61. Liu, R, Chan, DC: OPA1 and cardiolipin team up for mitochondrial fusion. *Nat Cell Biol,* 19**:** 760-762, 2017.
62. Pernas, L, Scorrano, L: Mito-Morphosis: Mitochondrial Fusion, Fission, and Cristae Remodeling as Key Mediators of Cellular Function. *Annu Rev Physiol,* 78**:** 505-531, 2016.
63. Bhargava, P, Schnellmann, RG: Mitochondrial energetics in the kidney. *Nat Rev Nephrol,* 13**:** 629-646, 2017.
64. Breitzig, MT, Alleyn, MD, Lockey, RF, Kolliputi, N: A mitochondrial delicacy: dynamin-related protein 1 and mitochondrial dynamics. *Am J Physiol Cell Physiol,* 315**:** C80-C90, 2018.
65. Li, T, Chen, ZJ: The cGAS-cGAMP-STING pathway connects DNA damage to inflammation, senescence, and cancer. *J Exp Med,* 215**:** 1287-1299, 2018.
66. Chung,KW, Dhillon, P, Huang, S, Sheng, X, Shrestha, R, Qiu, C, Kaufman, BA, Park, J, Pei, L, Baur, J, Palmer,M, Susztak, K: Mitochondrial Damage and Activation of the STING Pathway Lead to Renal Inflammation and Fibrosis. *Cell Metab*, 2019.
67. Madeo, F, Carmona-Gutierrez, D, Hofer, SJ, Kroemer, G: Caloric Restriction Mimetics against Age-Associated Disease: Targets, Mechanisms, and Therapeutic Potential. *Cell Metab,* 29**:** 592-610, 2019.
68. Sturmlechner, I, Durik, M, Sieben, CJ, Baker, DJ, van Deursen, JM: Cellular senescence in renal ageing and disease. *Nat Rev Nephrol,* 13**:** 77-89, 2017.
69. Valentijn, FA, Falke, LL, Nguyen, TQ, Goldschmeding, R: Cellular senescence in the aging and diseased kidney. *J Cell Commun Signal,* 12**:** 69-82, 2018.
70. Knoppert, SN, Valentijn, FA, Nguyen, TQ, Goldschmeding, R, Falke, LL: Cellular Senescence and the Kidney: Potential Therapeutic Targets and Tools. *Front Pharmacol,* 10**:** 770, 2019.
71. Docherty, MH, O'Sullivan, ED, Bonventre, JV, Ferenbach, DA: Cellular Senescence in the Kidney. *J Am Soc Nephrol,* 30**:** 726-736, 2019.
72. Ito, Y, Hoare, M, Narita, M: Spatial and Temporal Control of Senescence. *Trends Cell Biol,* 27**:** 820-832, 2017.
73. Fontana, L, Nehme, J, Demaria, M: Caloric restriction and cellular senescence. *Mech Ageing Dev,* 176**:** 19-23, 2018.
74. McHugh, D, Gil, J: Senescence and aging: Causes, consequences, and therapeutic avenues. *J Cell Biol,* 217**:** 65-77, 2018.
75. Ferrucci, L, Fabbri, E: Inflammageing: chronic inflammation in ageing, cardiovascular disease, and frailty. *Nat Rev Cardiol,* 15**:** 505-522, 2018.
76. Piber, D, Olmstead, R, Cho, JH, Witarama, T, Perez, C, Dietz, N, Seeman, TE, Breen, EC, Cole, SW, Irwin, MR: Inflammaging: Age and Systemic, Cellular, and Nuclear Inflammatory Biology in Older Adults. *J Gerontol A Biol Sci Med Sci*, 2019.
77. Fulop, T, Larbi, A, Witkowski, JM: Human Inflammaging. *Gerontology,* 65**:** 495-504, 2019.
78. Chung, HY, Kim, DH, Lee, EK, Chung, KW, Chung, S, Lee, B, Seo, AY, Chung, JH, Jung, YS, Im, E, Lee, J, Kim, ND, Choi, YJ, Im, DS, Yu, BP: Redefining Chronic

Inflammation in Aging and Age-Related Diseases: Proposal of the Senoinflammation Concept. *Aging Dis,* 10**:** 367-382, 2019.

79. Bang, E, Lee, B, Noh, SG, Kim, DH, Jung, HJ, Ha, S, Yu, BP, Chung, HY: Modulation of senoinflammation by calorie restriction based on biochemical and Omics big data analysis. *BMB Rep,* 52**:** 56-63, 2019.
80. Vringer, E, Tait, SWG: Mitochondria and Inflammation: Cell Death Heats Up. *Front Cell Dev Biol,* 7**:** 100, 2019.
81. Ablasser, A, Chen, ZJ: cGAS in action: Expanding roles in immunity and inflammation. *Science,* 363, 2019.
82. Ng, KW, Marshall, EA, Bell, JC, Lam, WL: cGAS-STING and Cancer: Dichotomous Roles in Tumor Immunity and Development. *Trends Immunol,* 39**:** 44-54, 2018.
83. Margolis, SR, Wilson, SC, Vance, RE: Evolutionary Origins of cGAS-STING Signaling. *Trends Immunol,* 38**:** 733-743, 2017.
84. Hsia, HC, Hutti, JE, Baldwin, AS: Cytosolic DNA Promotes Signal Transducer and Activator of Transcription 3 (STAT3) Phosphorylation by TANK-binding Kinase 1 (TBK1) to Restrain STAT3 Activity. *J Biol Chem,* 292**:** 5405-5417, 2017.
85. Kojima, H, Inoue, T, Kunimoto, H, Nakajima, K: IL-6-STAT3 signaling and premature senescence. *JAKSTAT,* 2**:** e25763, 2013.
86. Waters, DW, Blokland, KEC, Pathinayake, PS, Wei, L, Schuliga, M, Jaffar, J, Westall, GP, Hansbro, PM, Prele, CM, Mutsaers, SE, Bartlett, NW, Burgess, JK, Grainge, CL, Knight, DA: STAT3 Regulates the Onset of Oxidant-induced Senescence in Lung Fibroblasts. *Am J Respir Cell Mol Biol,* 61**:** 61-73, 2019.
87. Bienaime, F, Muorah, M, Yammine, L, Burtin, M, Nguyen, C, Baron, W, Garbay, S, Viau, A, Broueilh, M, Blanc, T, Peters, D, Poli, V, Anglicheau, D, Friedlander, G, Pontoglio, M, Gallazzini, M, Terzi, F: Stat3 Controls Tubulointerstitial Communication during CKD. *J Am Soc Nephrol,* 27**:** 3690-3705, 2016.
88. Pace, J, Paladugu, P, Das, B, He, JC, Mallipattu, SK: Targeting STAT3 signaling in kidney disease. *Am J Physiol Renal Physiol,* 316**:** F1151-F1161, 2019.
89. Jiang, T, Wang, XX, Scherzer, P, Wilson, P, Tallman, J, Takahashi, H, Li, J, Iwahashi, M, Sutherland, E, Arend, L, Levi, M: Farnesoid X receptor modulates renal lipid metabolism, fibrosis, and diabetic nephropathy. *Diabetes,* 56**:** 2485-2493, 2007.
90. Wang, XX, Jiang, T, Shen, Y, Caldas, Y, Miyazaki-Anzai, S, Santamaria, H, Urbanek, C, Solis, N, Scherzer, P, Lewis, L, Gonzalez, FJ, Adorini, L, Pruzanski, M, Kopp, JB, Verlander, JW, Levi, M: Diabetic nephropathy is accelerated by farnesoid X receptor deficiency and inhibited by farnesoid X receptor activation in a type 1 diabetes model. *Diabetes,* 59**:** 2916-2927, 2010.
91. Wang, XX, Edelstein, MH, Gafter, U, Qiu, L, Luo, Y, Dobrinskikh, E, Lucia, S, Adorini, L, D'Agati, VD, Levi, J, Rosenberg, A, Kopp, JB, Gius, DR, Saleem, MA, Levi, M: G Protein-Coupled Bile Acid Receptor TGR5 Activation Inhibits Kidney Disease in Obesity and Diabetes. *J Am Soc Nephrol,* 27**:** 1362-1378, 2016.
92. Wang, XX, Jiang, T, Shen, Y, Adorini, L, Pruzanski, M, Gonzalez, FJ, Scherzer, P, Lewis, L, Miyazaki-Anzai, S, Levi, M: The farnesoid X receptor modulates renal lipid metabolism and diet-induced renal inflammation, fibrosis, and proteinuria. *Am J Physiol Renal Physiol,* 297**:** F1587-1596, 2009.

93. Zhang, X, Nguyen, KD, Rudnick, PA, Roper, N, Kawaler, E, Maity, TK, Awasthi, S, Gao, S, Biswas, R, Venugopalan, A, Cultraro, CM, Fenyo, D, Guha, U: Quantitative Mass Spectrometry to Interrogate Proteomic Heterogeneity in Metastatic Lung Adenocarcinoma and Validate a Novel Somatic Mutation CDK12-G879V. *Mol Cell Proteomics,* 18**:** 622-641, 2019.
94. Cox, J, Mann, M: MaxQuant enables high peptide identification rates, individualized p.p.b.-range mass accuracies and proteome-wide protein quantification. *Nat Biotechnol,* 26**:** 1367-1372, 2008.
95. Cox, J, Neuhauser, N, Michalski, A, Scheltema, RA, Olsen, JV, Mann, M: Andromeda: a peptide search engine integrated into the MaxQuant environment. *J Proteome Res,* 10**:** 1794-1805, 2011.
96. Hao, H, Cao, L, Jiang, C, Che, Y, Zhang, S, Takahashi, S, Wang, G, Gonzalez, FJ: Farnesoid X Receptor Regulation of the NLRP3 Inflammasome Underlies Cholestasis-Associated Sepsis. *Cell Metab,* 25**:** 856-867 e855, 2017.
97. Prasun, P, Young, S, Salomons, G, Werneke, A, Jiang, YH, Struys, E, Paige, M, Avantaggiati, ML, McDonald, M: Expanding the Clinical Spectrum of Mitochondrial Citrate Carrier (SLC25A1) Deficiency: Facial Dysmorphism in Siblings with Epileptic Encephalopathy and Combined D,L-2-Hydroxyglutaric Aciduria. *JIMD Rep,* 19**:** 111-115, 2015.
98. Jiang, C, Xie, C, Lv, Y, Li, J, Krausz, KW, Shi, J, Brocker, CN, Desai, D, Amin, SG, Bisson, WH, Liu, Y, Gavrilova, O, Patterson, AD, Gonzalez, FJ: Intestine-selective farnesoid X receptor inhibition improves obesity-related metabolic dysfunction. *Nat Commun,* 6**:** 10166, 2015.
99. Takahashi, S, Tanaka, N, Fukami, T, Xie, C, Yagai, T, Kim, D, Velenosi, TJ, Yan, T, Krausz, KW, Levi, M, Gonzalez, FJ: Role of Farnesoid X Receptor and Bile Acids in Hepatic Tumor Development. *Hepatol Commun,* 2**:** 1567-1582, 2018.
100. Takahashi, S, Tanaka, N, Golla, S, Fukami, T, Krausz, KW, Polunas, MA, Weig, BC, Masuo, Y, Xie, C, Jiang, C, Gonzalez, FJ: Editor's Highlight: Farnesoid X Receptor Protects Against Low-Dose Carbon Tetrachloride-Induced Liver Injury Through the Taurocholate-JNK Pathway. *Toxicol Sci,* 158**:** 334-346, 2017.
101. Tanaka, N, Matsubara, T, Krausz, KW, Patterson, AD, Gonzalez, FJ: Disruption of phospholipid and bile acid homeostasis in mice with nonalcoholic steatohepatitis. *Hepatology,* 56**:** 118-129, 2012.
102. Tsugawa, H, Nakabayashi, R, Mori, T, Yamada, Y, Takahashi, M, Rai, A, Sugiyama, R, Yamamoto, H, Nakaya, T, Yamazaki, M, Kooke, R, Bac-Molenaar, JA, Oztolan-Erol, N, Keurentjes, JJB, Arita, M, Saito, K: A cheminformatics approach to characterize metabolomes in stable-isotope-labeled organisms. *Nat Methods,* 16**:** 295-298, 2019.
103. Tsugawa, H, Cajka, T, Kind, T, Ma, Y, Higgins, B, Ikeda, K, Kanazawa, M, VanderGheynst, J, Fiehn, O, Arita, M: MS-DIAL: data-independent MS/MS deconvolution for comprehensive metabolome analysis. *Nat Methods,* 12**:** 523-526, 2015.
104. Bouhaddani, SE, Uh, HW, Jongbloed, G, Hayward, C, Klaric, L, Kielbasa, SM, Houwing-Duistermaat, J: Integrating omics datasets with the OmicsPLS package. *BMC Bioinformatics,* 19**:** 371, 2018.

Supplementary Table 1:

A. List of primers

Name	Forward	Reverse
Esrrα	CAGGGAGGGAAGGGATGG	ATGAGGAGAGGAGCGAAGG
Esrrb	GCACCTGGGCTCTAGTTGC	TACAGTCCTCGTAGCTCTTGC
Esrrg	AAGATCGACACATTGATTCCAGC	CATGGTTGAACTGTAACTCCCAC
Ppargc1a	GTCAGAGTGGATTGGAGTTG	AAGTCATTCACATCAAGTTCAG
Ppargc1b	TCCTGTAAAAGCCCGGAGTAT	GCTCTGGTAGGGGCAGTGA
Pdk4	AGGGAGGTCGAGCTGTTCTC	GGAGTGTTCACTAAGCGGTCA
Acadm	AACACTTACTATGCCTCGATTGCA	CCATAGCCTCCGAAAATCTGAA
Tfam1	AACACCCAGATGCAAAACTTTCA	GACTTGGAGTTAGCTGCTCTTT
mtDNA	ATAACCGAGTCGTTCTGCCAAT	TTTCAGAGCATTGGCCATAGAA
Sdhc	GCTGCGTTCTTGCTGAGACA	ATCTCCTCCTTAGCTGTGGTT
Atp5b	GGTTCATCCTGCCAGAGACTA	AATCCCTCATCGAACTGGACG
Pdhb	AGGAGGGAATTGAATGTGAGGT	ACTGGCTTCTATGGCTTCGAT
Mdh1	TTCTGGACGGTGTCCTGATG	TTTCACATTGGCTTTCAGTAGGT
Idh3b	TGGAGAGGTCTCGGAACATCT	AGCCTTGAACACTTCCTTGAC
Sucla2	ACCCTTTCGCTGCATGAATAC	CCTGTGCCTTTATCACAACATCC
Cpt1a	CTCCGCCTGAGCCATGAAG	CACCAGTGATGATGCCATTCT
Ndufb8	TGTTGCCGGGGTCATATCCTA	AGCATCGGGTAGTCGCCATA
Opa1	CGACTTTGCCGAGGATAGCTT	CGTTGTGAACACACTGCTCTTG
Miga2	GGAGGACTGAGGGTATGTCCA	CAAGGGCTGTGGCAAAAAGA
Pld6	ACCTGCACCGAGGCTTTAC	CATGTAGTCGCAGTCAGTGATG
Il1b	GCAACTGTTCCTGAACTCAACT	ATCTTTTGGGGTCCGTCAACT
Icam1	GTGATGCTCAGGTATCCATCCA	CACAGTTCTCAAAGCACAGCG
Stat3	AGCTGGACACACGCTACCT	AGGAATCGGCTATATTGCTGGT
Uqcrb	GGCCGATCTGCTGTTTCAG	CATCTCGCATTAACCCCAGTT
Cox6a2	CTGCTCCCTTAACTGCTGGAT	GATTGTGGAAAAGCGTGTGGT
Tmem173	GGTCACCGCTCCAAATATGTAG	CAGTAGTCCAAGTTCGTGCGA
Cdkn1a	CCTGGTGATGTCCGACCTG	CCATGAGCGCATCGCAATC

B. Antibodies

Name	Host	Source	Catalogue Number
OPA1	Mouse	BD Biosciences	612606
MFN2	Rabbit	Millipore	978-715-4321
DRP1	Mouse	Novusbio	H00010059-M01
p-DRP1 (s616)	Rabbit	Cell Signaling	3455S
Stat3	Rabbit	Cell Signaling	4904T
p-Stat3 (Y705)	Rabbit	Cell Signaling	9145T
PDH e2/e3	Mouse	Abcam	

Figure 1

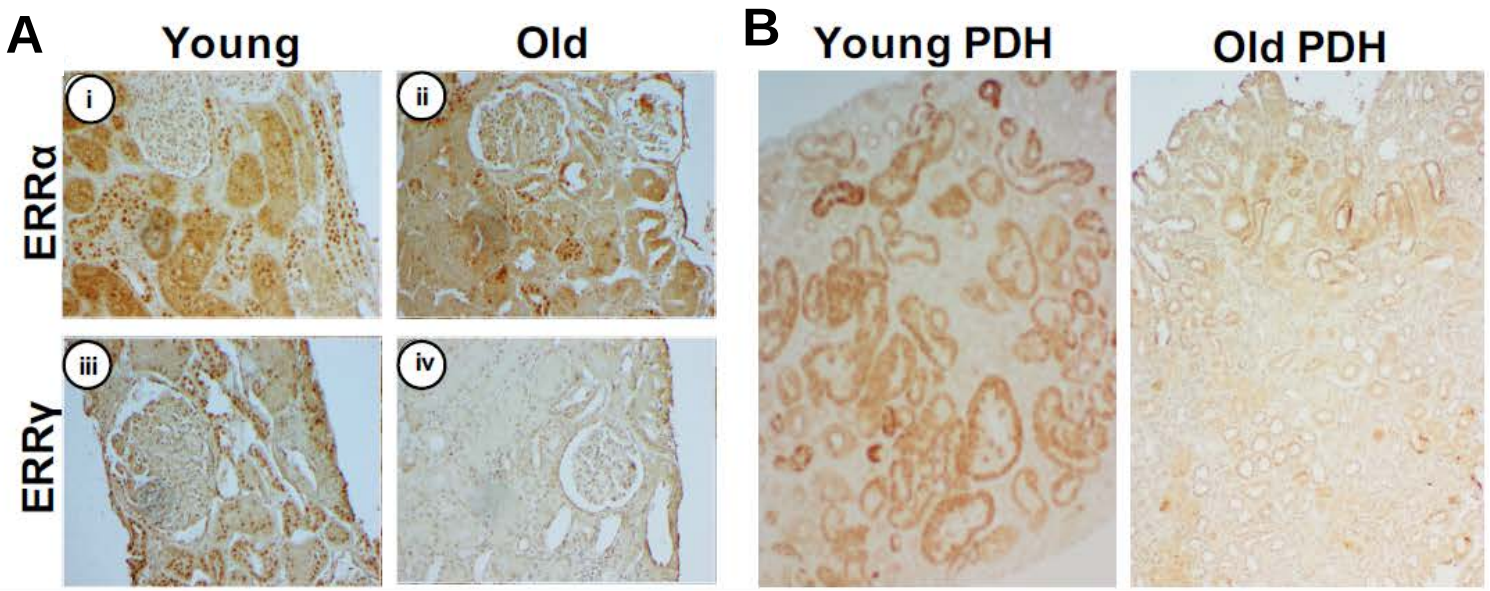

Figure 2

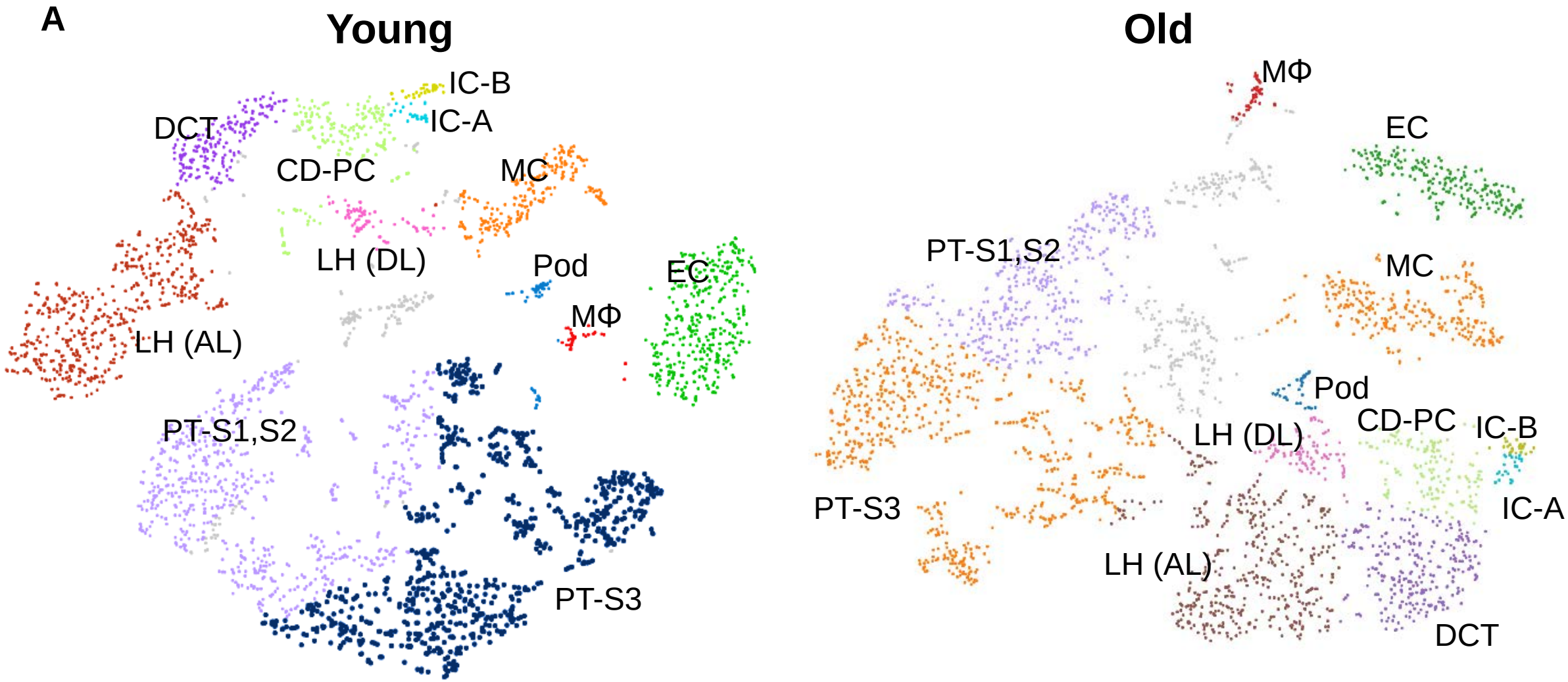
A
Young
IC-B
IC-A
DCT
CD-PC
MC
LH (DL)
Pod
EC
MΦ
LH (AL)
PT-S1,S2
PT-S3
Old
MΦ
EC
PT-S1,S2
MC
Pod
CD-PC
IC-B
LH (DL)
PT-S3
IC-A
LH (AL)
DCT

Figure 2

B

% of ERRα positive cells in each cluster			
	Young	Old	
Pod	27	14	
MC	8	7	
EC	4	5	
MΦ	4	4	
DCT	15	10	
LH-AL	21	17	
LH-DL	11	8	
IC-B	41	25	
IC-A	27	12	
CD-PC	12	13	
PT-S3	32	28	
PT-S1/S2	30	19	

% of ERRγ positive cells in each cluster			
	Young	Old	
Pod	0	12	
MC	1	1	
EC	1	1	
MΦ	0	0	
DCT	4	4	
LH-AL	3	6	
LH-DL	3	3	
IC-B	0	7	
IC-A	8	0	
CD-PC	1	4	
PT-S3	7	6	
PT-S1/S2	6	3	

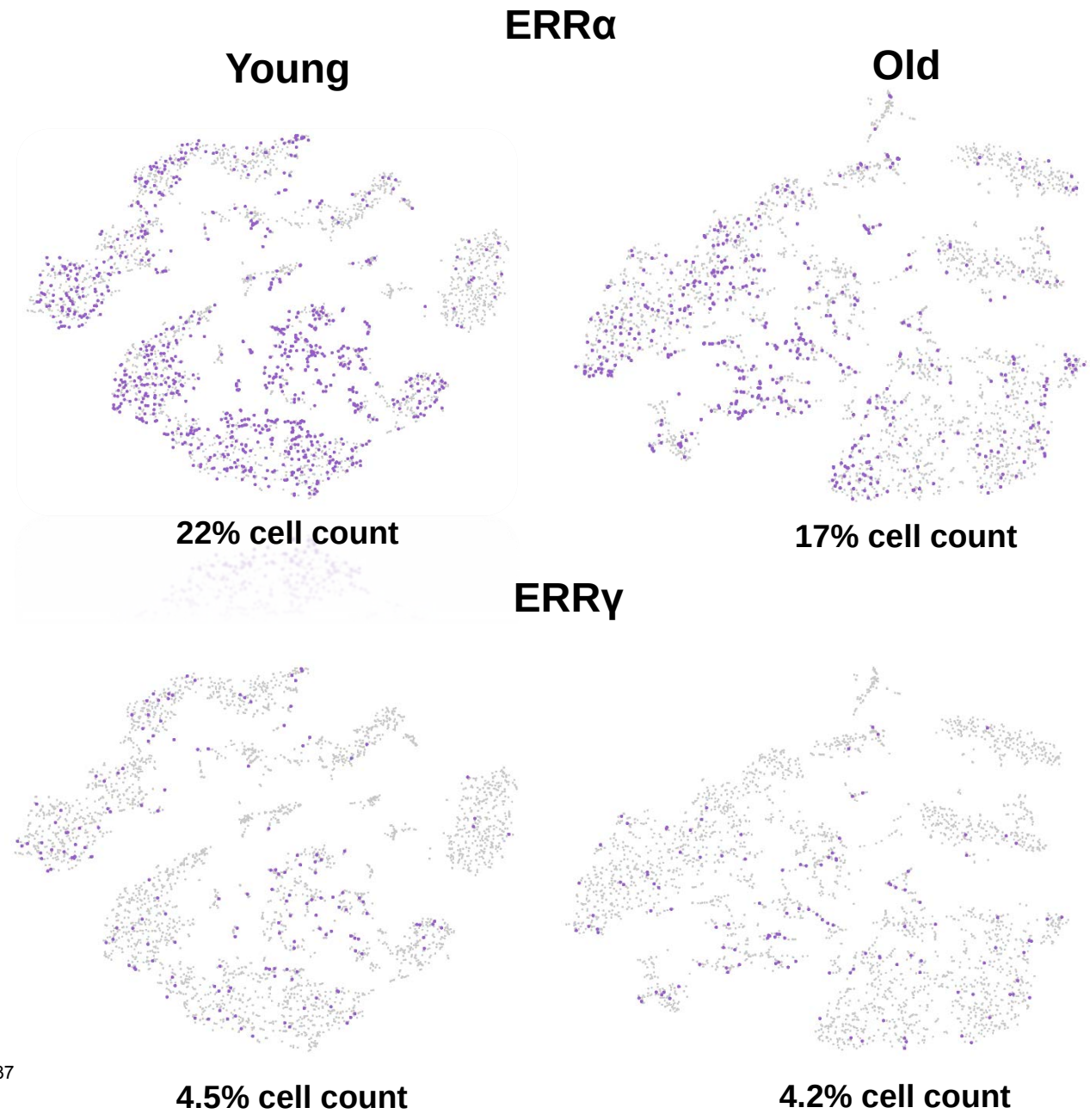

Figure 3

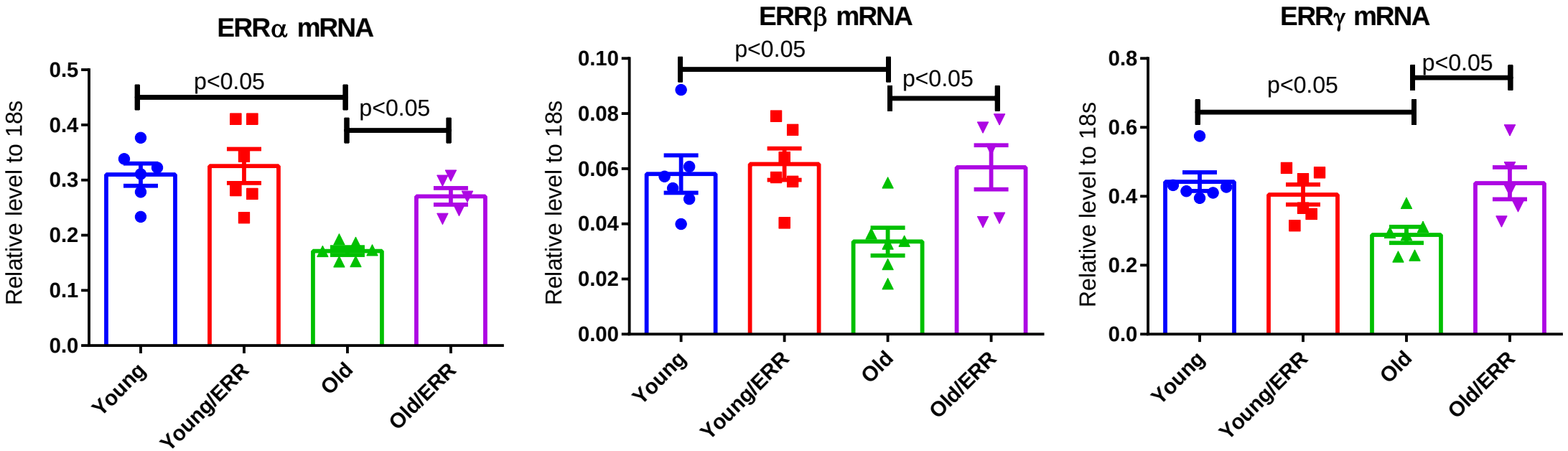
ERRα mRNA
Relative level to 18s
0.5
0.4
0.3
0.2
0.1
0.0
p<0.05
p<0.05
Young
Young/ERR
Old
Old/ERR
ERRβ mRNA
Relative level to 18s
0.10
0.08
0.06
0.04
0.02
0.00
p<0.05
p<0.05
Young
Young/ERR
Old
Old/ERR
ERRγ mRNA
Relative level to 18s
0.8
0.6
0.4
0.2
0.0
p<0.05
p<0.05
Young
Young/ERR
Old
Old/ERR

Figure 4

A

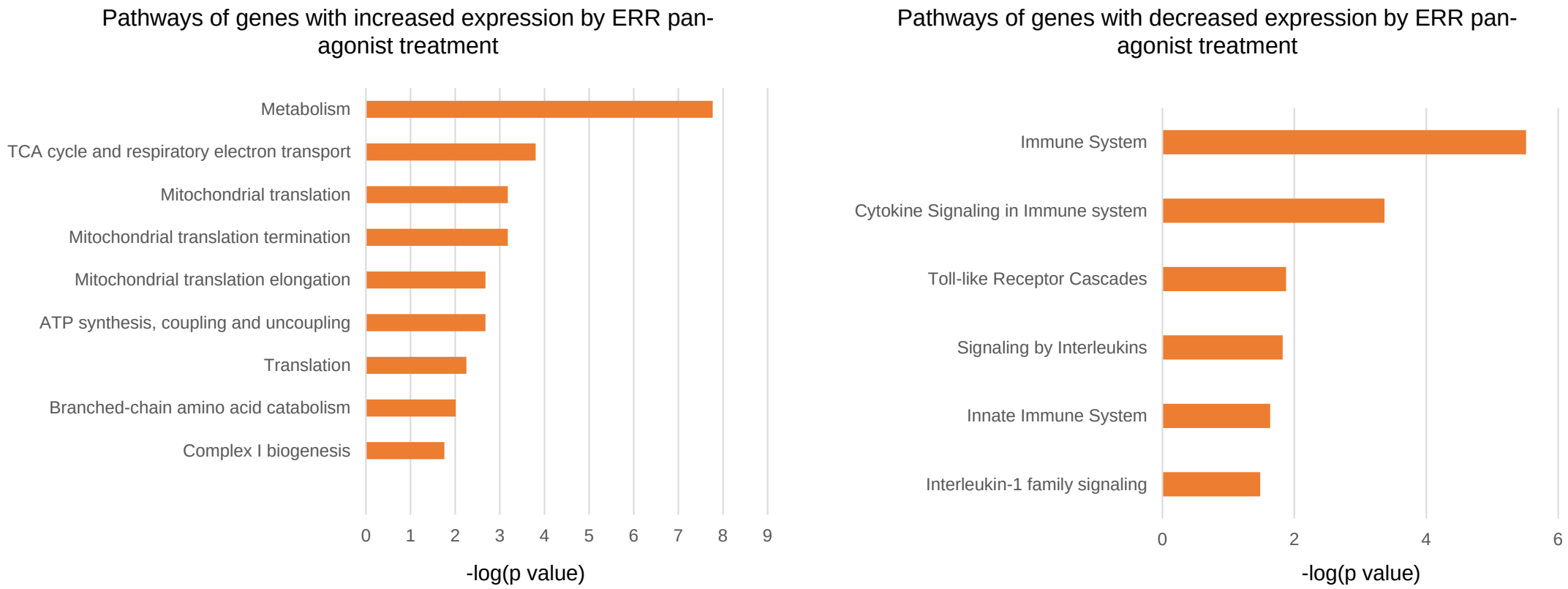
Pathways of genes with increased expression by ERR pan-agonist treatment
Metabolism
TCA cycle and respiratory electron transport
Mitochondrial translation
Mitochondrial translation termination
Mitochondrial translation elongation
ATP synthesis, coupling and uncoupling
Translation
Branched-chain amino acid catabolism
Complex I biogenesis
0
1
2
3
4
5
6
7
8
9
-log(p value)
Pathways of genes with decreased expression by ERR pan-agonist treatment
Immune System
Cytokine Signaling in Immune system
Toll-like Receptor Cascades
Signaling by Interleukins
Innate Immune System
Interleukin-1 family signaling
0
2
4
6
-log(p value)

Figure 4

B

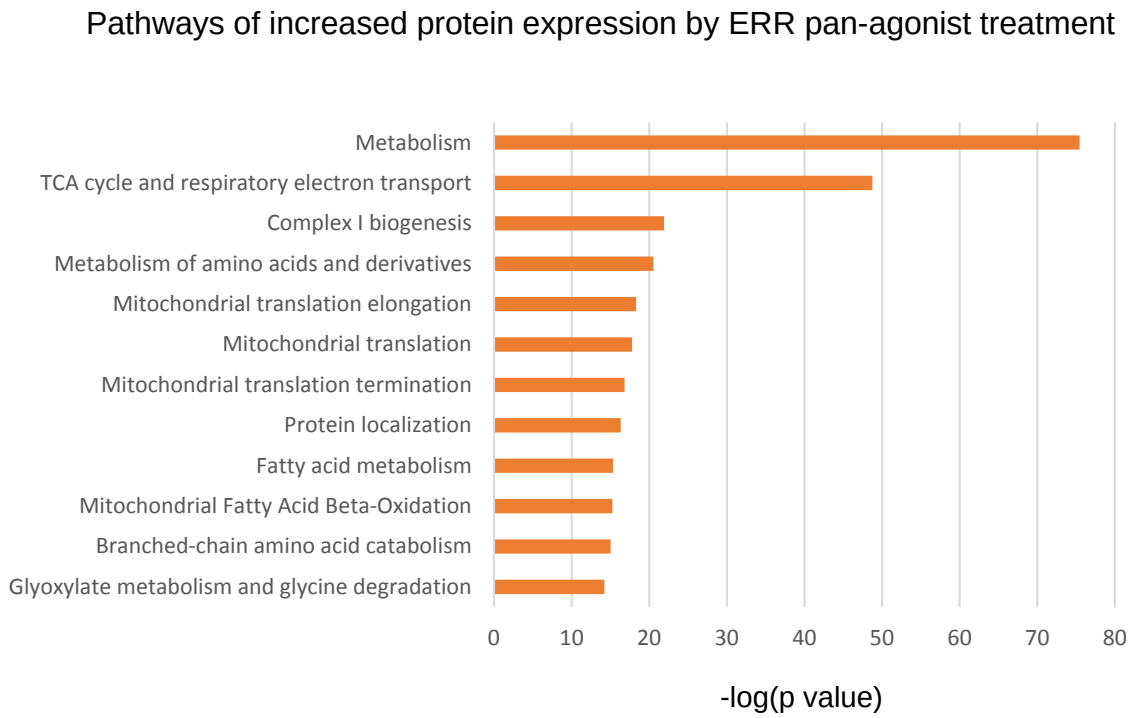
Pathways of increased protein expression by ERR pan-agonist treatment
Metabolism
TCA cycle and respiratory electron transport
Complex I biogenesis
Metabolism of amino acids and derivatives
Mitochondrial translation elongation
Mitochondrial translation
Mitochondrial translation termination
Protein localization
Fatty acid metabolism
Mitochondrial Fatty Acid Beta-Oxidation
Branched-chain amino acid catabolism
Glyoxylate metabolism and glycine degradation
0
10
20
30
40
50
60
70
80
-log(p value)

Figure 4

C

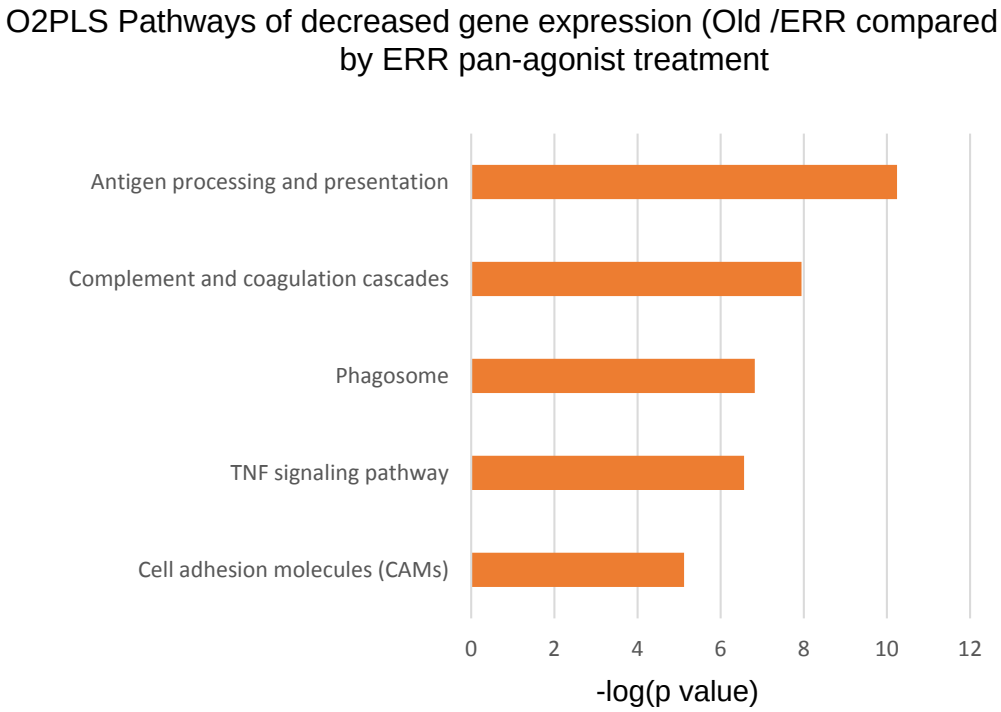
O2PLS Pathways of decreased gene expression (Old /ERR compared to Old) by ERR pan-agonist treatment
Antigen processing and presentation
Complement and coagulation cascades
Phagosome
TNF signaling pathway
Cell adhesion molecules (CAMs)
0
2
4
6
8
10
12
-log(p value)

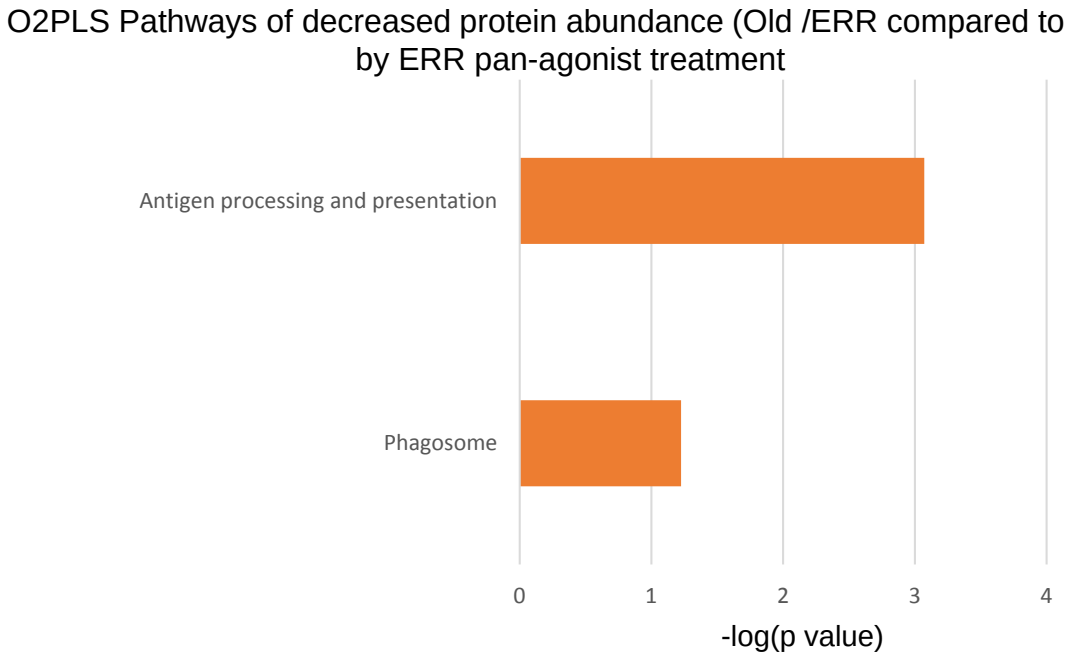
O2PLS Pathways of decreased protein abundance (Old /ERR compared to Old) by ERR pan-agonist treatment
Antigen processing and presentation
Phagosome
0
1
2
3
4
-log(p value)

Figure 5

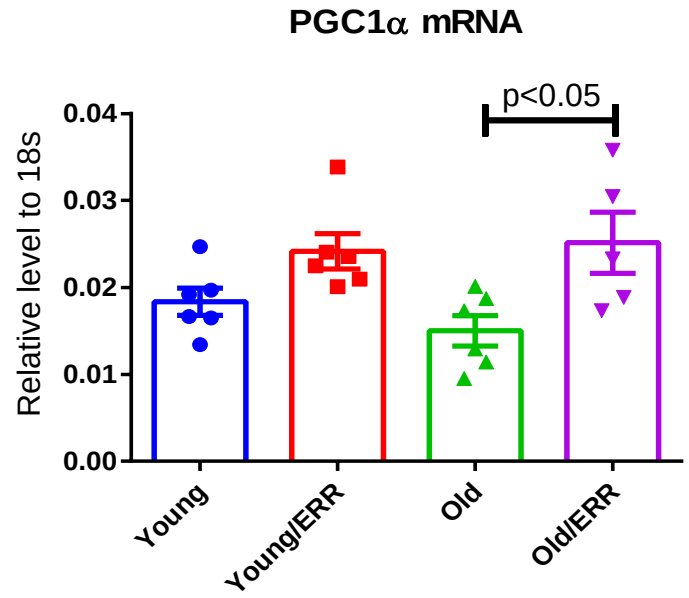
PGC1α mRNA
p<0.05
Relative level to 18s
0.04
0.03
0.02
0.01
0.00
Young
Young/ERR
Old
Old/ERR

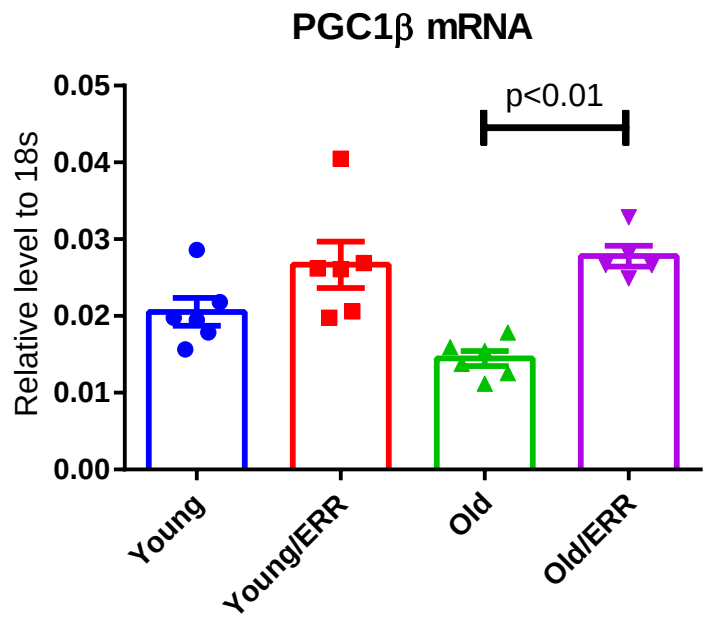
PGC1β mRNA
p<0.01
Relative level to 18s
0.05
0.04
0.03
0.02
0.01
0.00
Young
Young/ERR
Old
Old/ERR

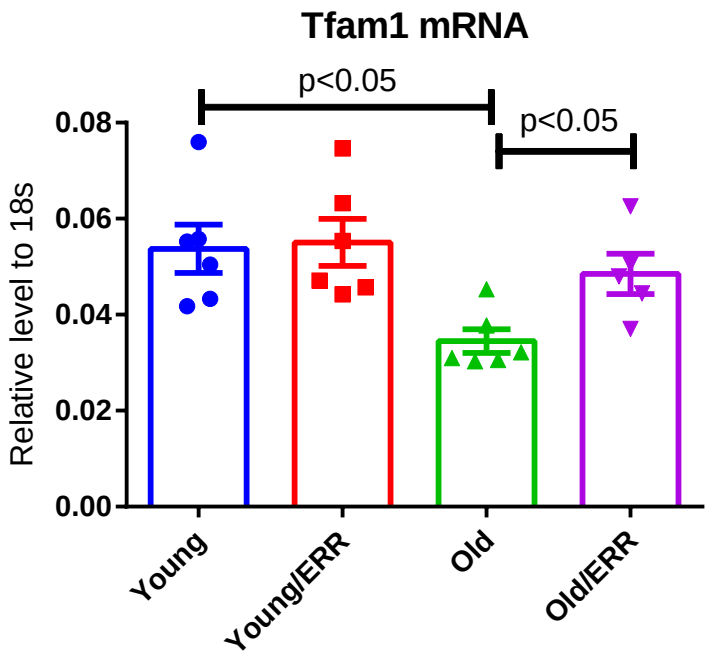
Tfam1 mRNA
p<0.05
p<0.05
Relative level to 18s
0.08
0.06
0.04
0.02
0.00
Young
Young/ERR
Old
Old/ERR

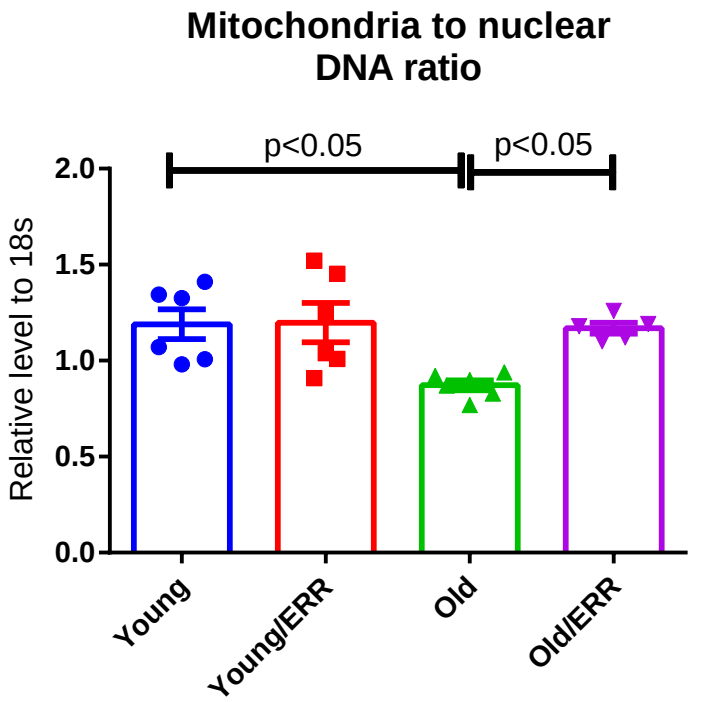
Mitochondria to nuclear DNA ratio
p<0.05
p<0.05
Relative level to 18s
2.0
1.5
1.0
0.5
0.0
Young
Young/ERR
Old
Old/ERR

Figure 6

A

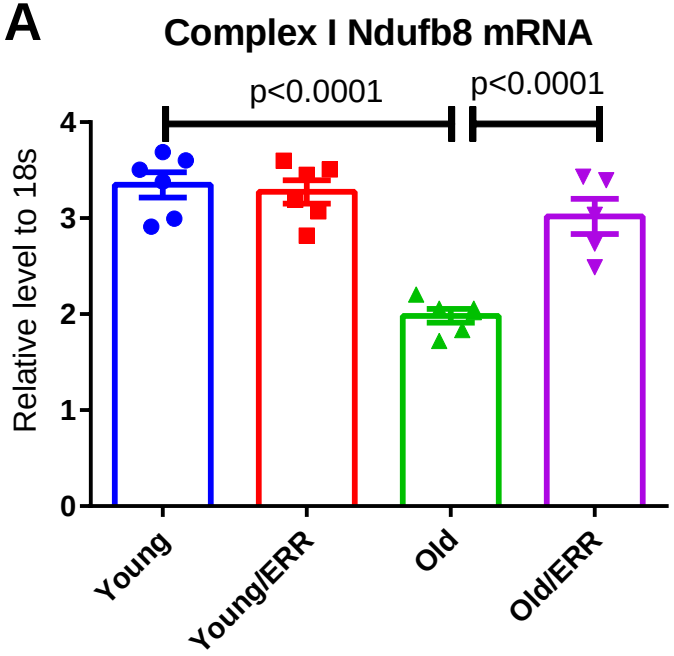
Complex I Ndufb8 mRNA
p<0.0001
p<0.0001
Relative level to 18s
0
1
2
3
4
Young
Young/ERR
Old
Old/ERR

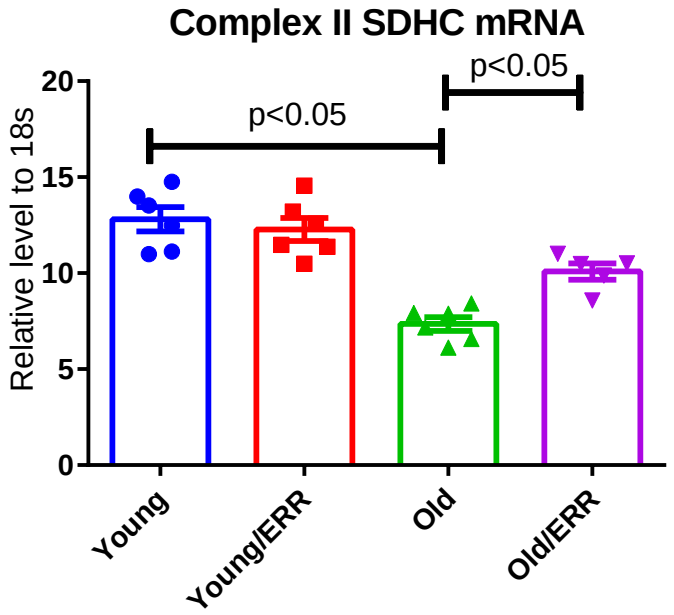
Complex II SDHC mRNA
p<0.05
p<0.05
Relative level to 18s
0
5
10
15
20
Young
Young/ERR
Old
Old/ERR

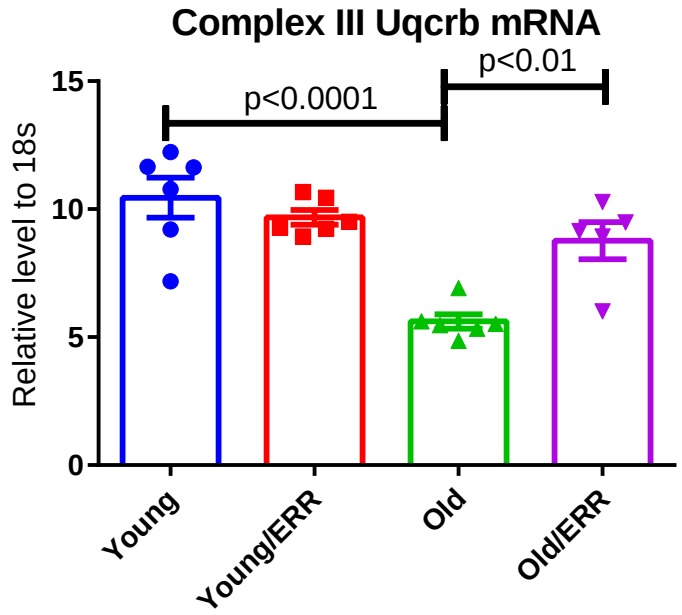
Complex III Uqcrb mRNA
p<0.01
p<0.0001
Relative level to 18s
0
5
10
15
Young
Young/ERR
Old
Old/ERR

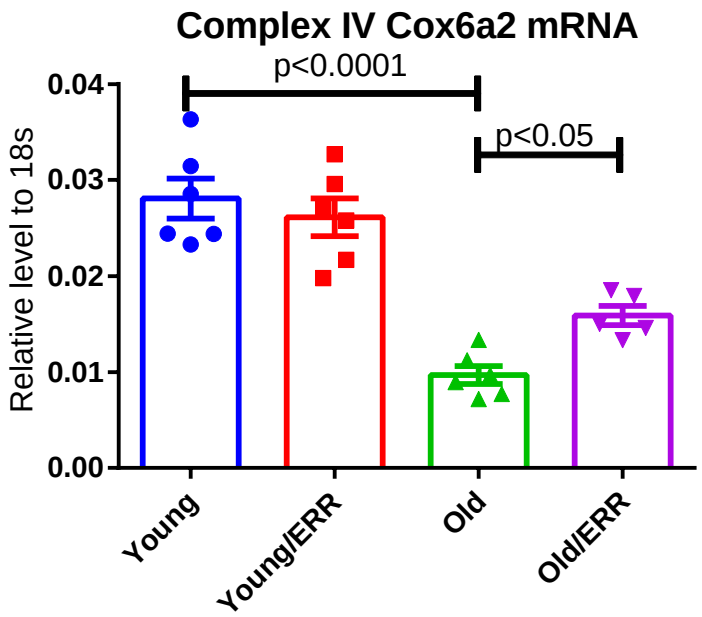
Complex IV Cox6a2 mRNA
p<0.0001
p<0.05
Relative level to 18s
0.00
0.01
0.02
0.03
0.04
Young
Young/ERR
Old
Old/ERR

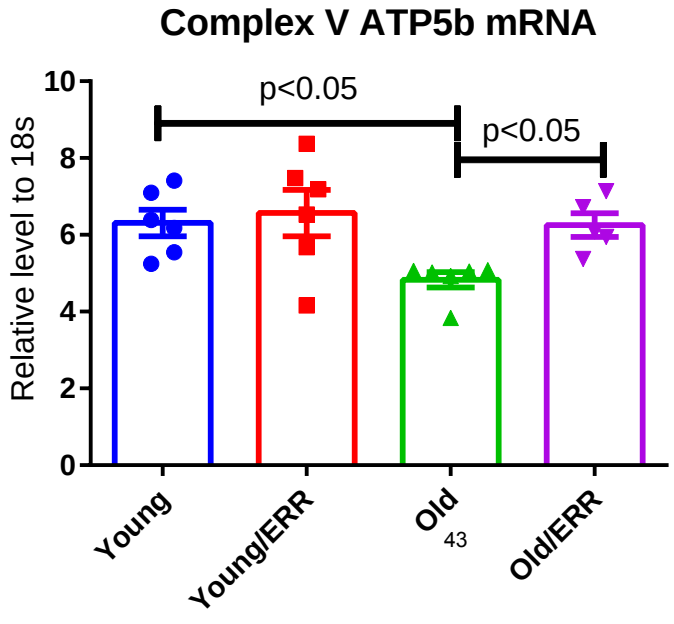
Complex V ATP5b mRNA
p<0.05
p<0.05
Relative level to 18s
0
2
4
6
8
10
Young
Young/ERR
Old
Old/ERR

Figure 6

B

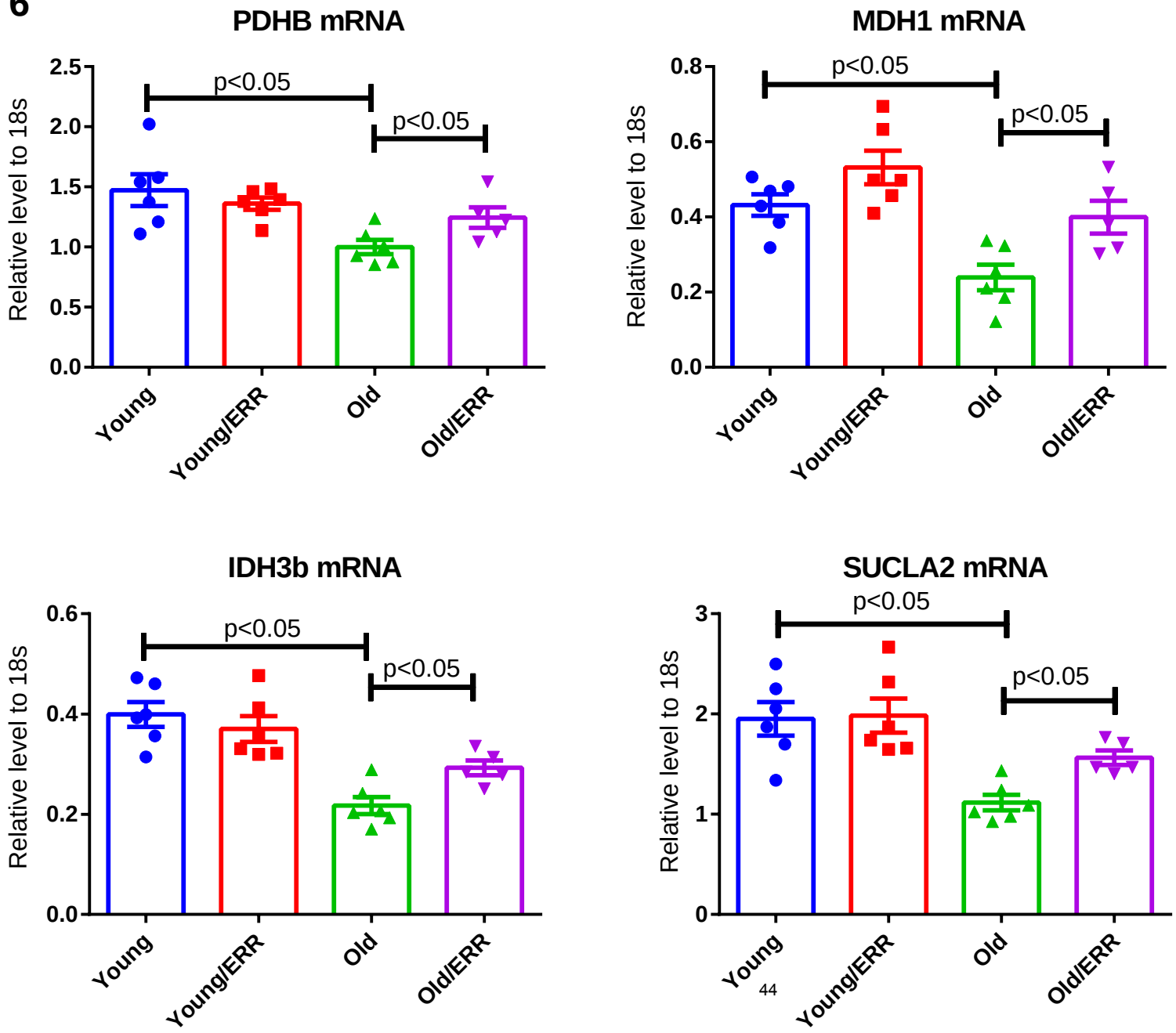
PDHB mRNA
Relative level to 18s
2.5
2.0
1.5
1.0
0.5
0.0
p<0.05
p<0.05
Young
Young/ERR
Old
Old/ERR
MDH1 mRNA
Relative level to 18s
0.8
0.6
0.4
0.2
0.0
p<0.05
p<0.05
Young
Young/ERR
Old
Old/ERR
IDH3b mRNA
Relative level to 18s
0.6
0.4
0.2
0.0
p<0.05
p<0.05
Young
Young/ERR
Old
Old/ERR
SUCLA2 mRNA
Relative level to 18s
3
2
1
0
p<0.05
p<0.05
Young
Young/ERR
Old
Old/ERR

Figure 6

C

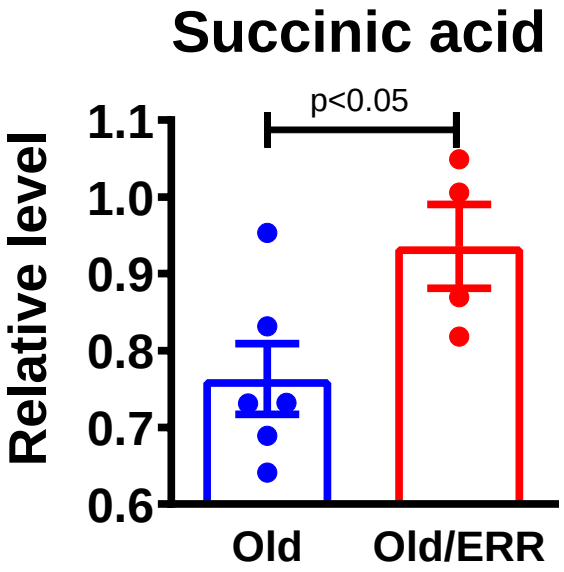
Succinic acid
p<0.05
Relative level
1.1
1.0
0.9
0.8
0.7
0.6
Old
Old/ERR

D

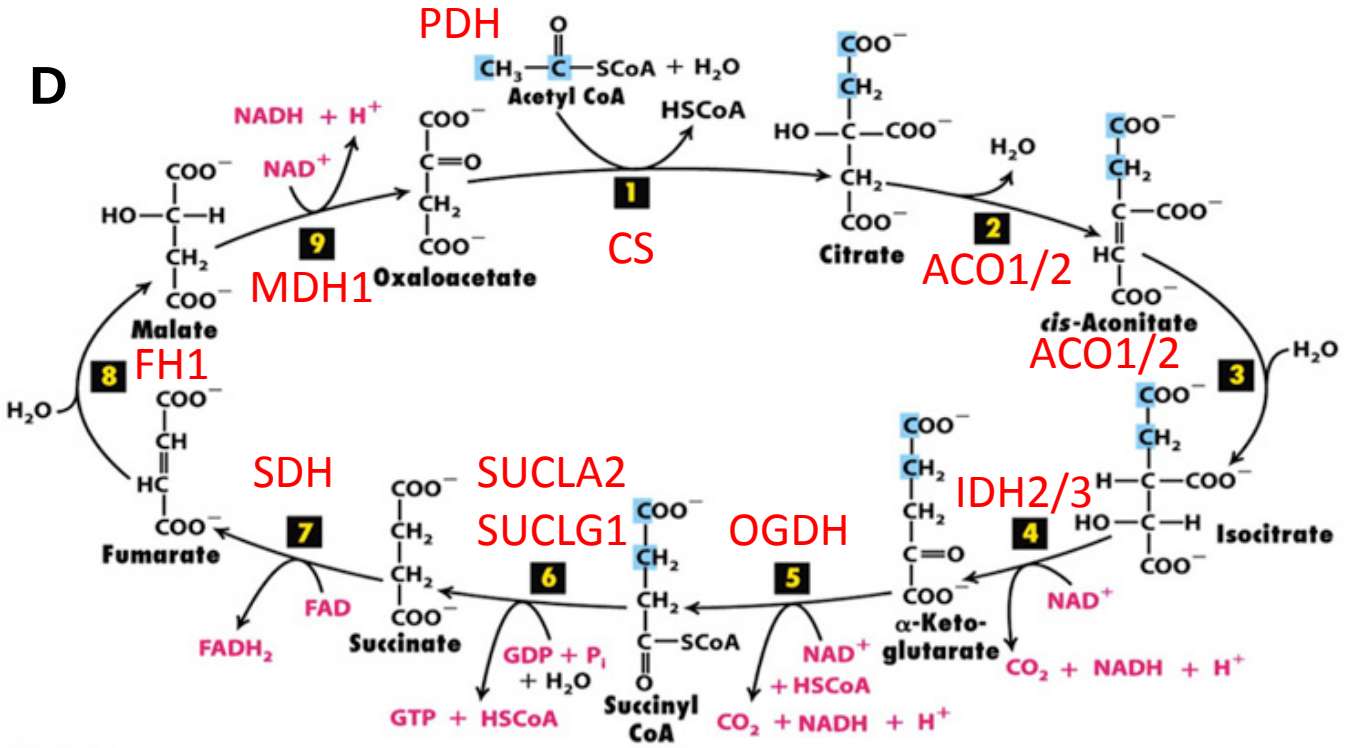
PDH
Acetyl CoA
HSCoA
NADH + H+
NAD+
Oxaloacetate
CS
Citrate
ACO1/2
cis-Aconitate
ACO1/2
Isocitrate
IDH2/3
NAD+
CO2 + NADH + H+
α-Keto-glutarate
OGDH
NAD+ + HSCoA
CO2 + NADH + H+
Succinyl CoA
SUCLA2
SUCLG1
GDP + Pi + H2O
GTP + HSCoA
Succinate
SDH
FAD
FADH2
Fumarate
FH1
H2O
Malate
MDH1

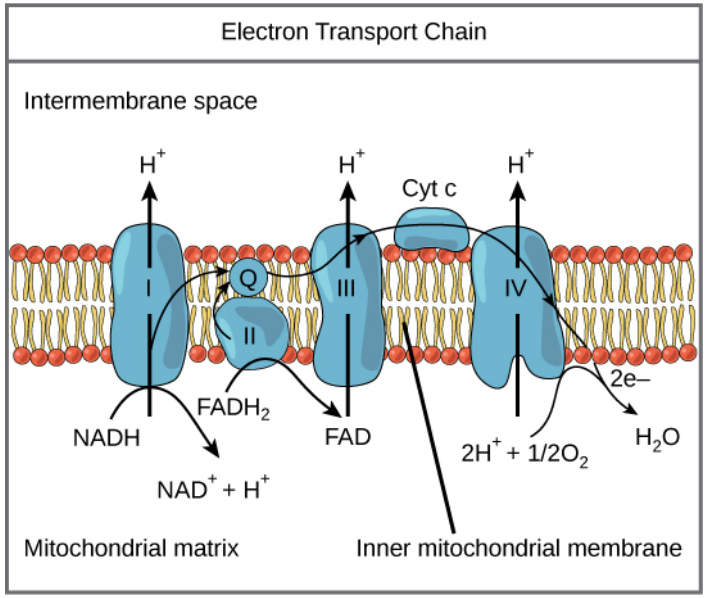
Electron Transport Chain
Intermembrane space
H+
H+
H+
Cyt c
I
II
Q
III
IV
NADH
FADH2
FAD
2e–
2H+ + 1/2O2
H2O
NAD+ + H+
Mitochondrial matrix
Inner mitochondrial membrane

Figure 7

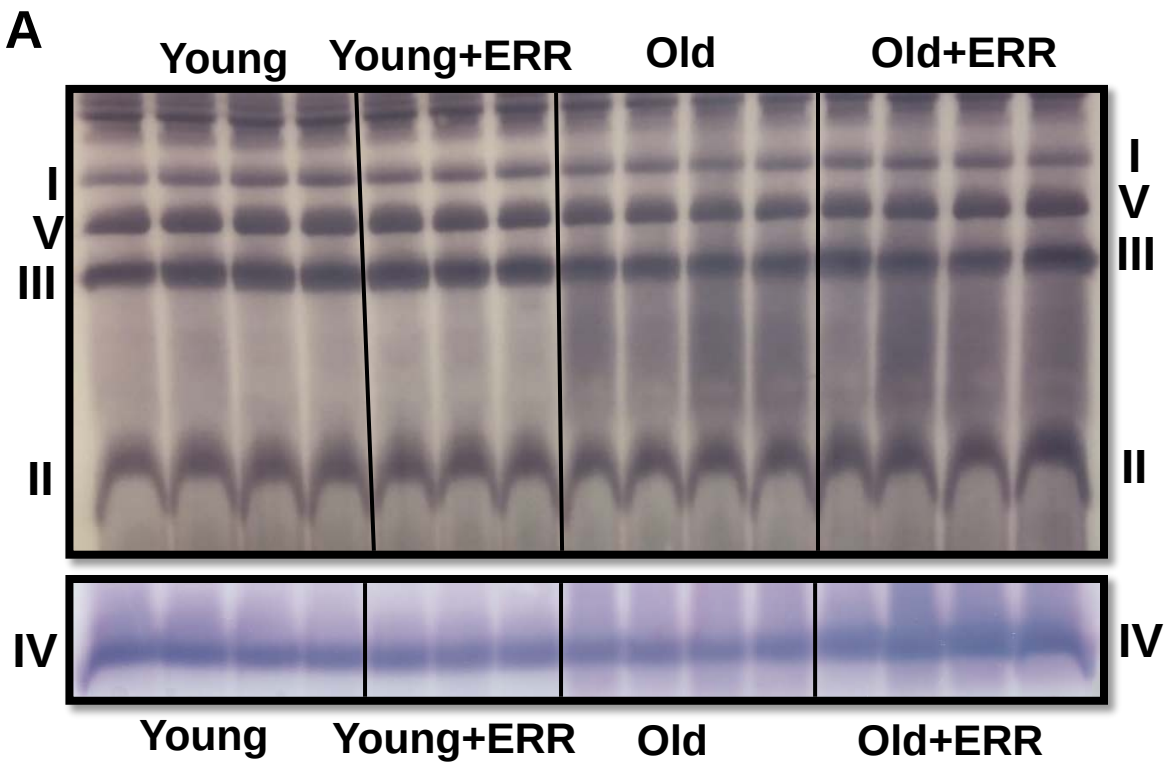
A
Young
Young+ERR
Old
Old+ERR
I
V
III
II
IV
Young
Young+ERR
Old
Old+ERR

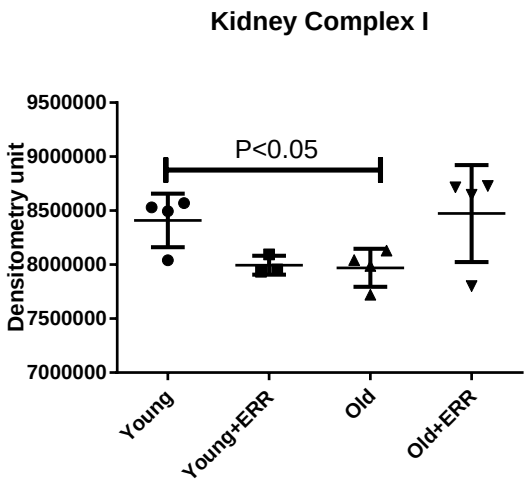
Kidney Complex I
Densitometry unit
9500000
9000000
8500000
8000000
7500000
7000000
P<0.05
Young
Young+ERR
Old
Old+ERR

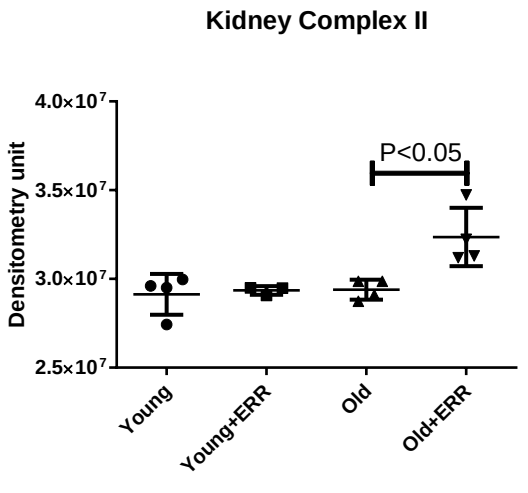
Kidney Complex II
Densitometry unit
4.0×10⁷
3.5×10⁷
3.0×10⁷
2.5×10⁷
P<0.05
Young
Young+ERR
Old
Old+ERR

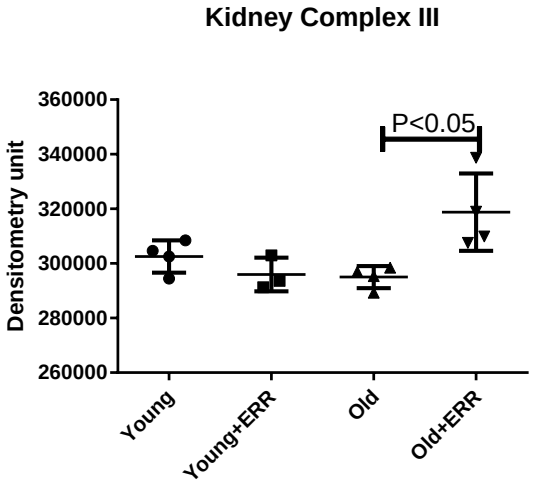
Kidney Complex III
Densitometry unit
360000
340000
320000
300000
280000
260000
P<0.05
Young
Young+ERR
Old
Old+ERR

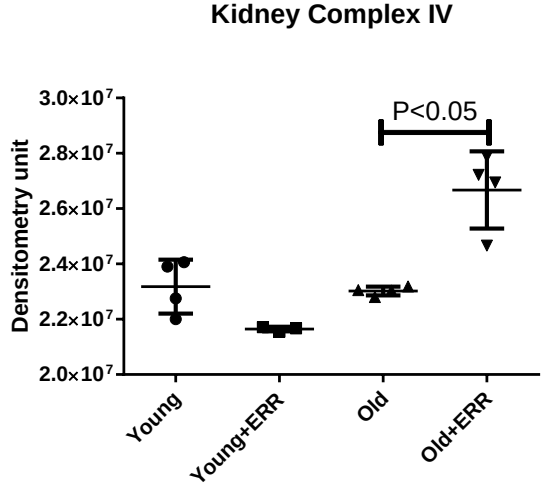
Kidney Complex IV
Densitometry unit
3.0×10⁷
2.8×10⁷
2.6×10⁷
2.4×10⁷
2.2×10⁷
2.0×10⁷
P<0.05
Young
Young+ERR
Old
Old+ERR

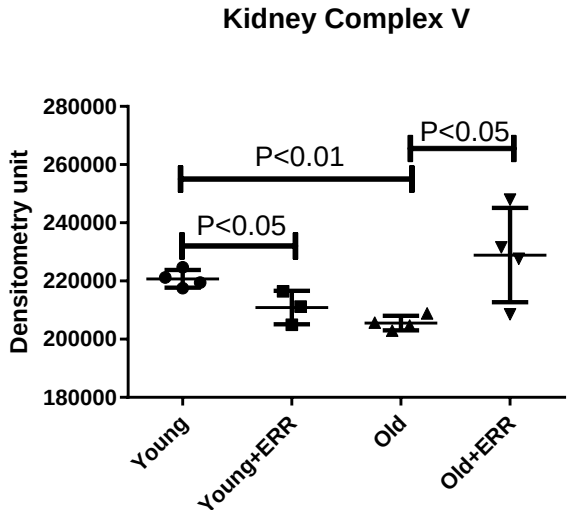
Kidney Complex V
Densitometry unit
280000
260000
240000
220000
200000
180000
P<0.01
P<0.05
P<0.05
Young
Young+ERR
Old
Old+ERR

Figure 7

B

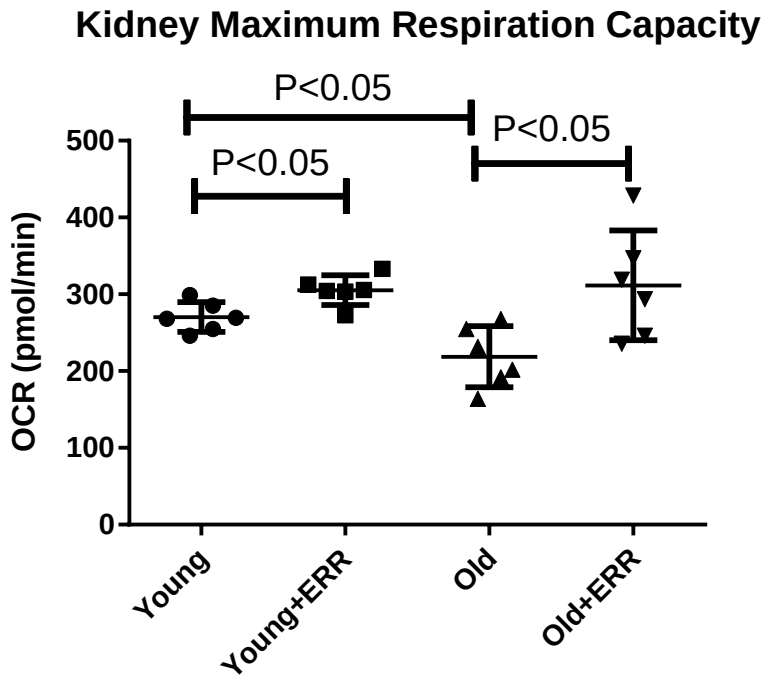
Kidney Maximum Respiration Capacity
P<0.05
P<0.05
P<0.05
OCR (pmol/min)
500
400
300
200
100
0
Young
Young+ERR
Old
Old+ERR

Figure 8

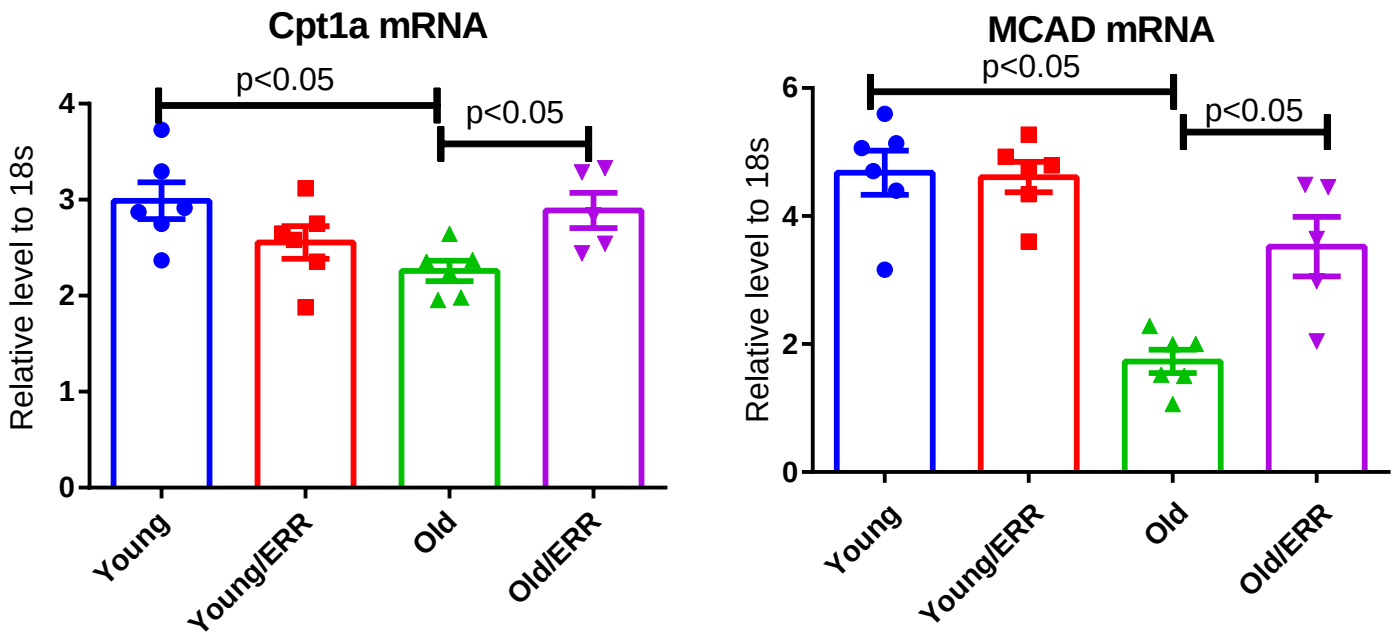
Cpt1a mRNA
p<0.05
p<0.05
Relative level to 18s
0
1
2
3
4
Young
Young/ERR
Old
Old/ERR
MCAD mRNA
p<0.05
p<0.05
Relative level to 18s
0
2
4
6
Young
Young/ERR
Old
Old/ERR

Figure 9

A

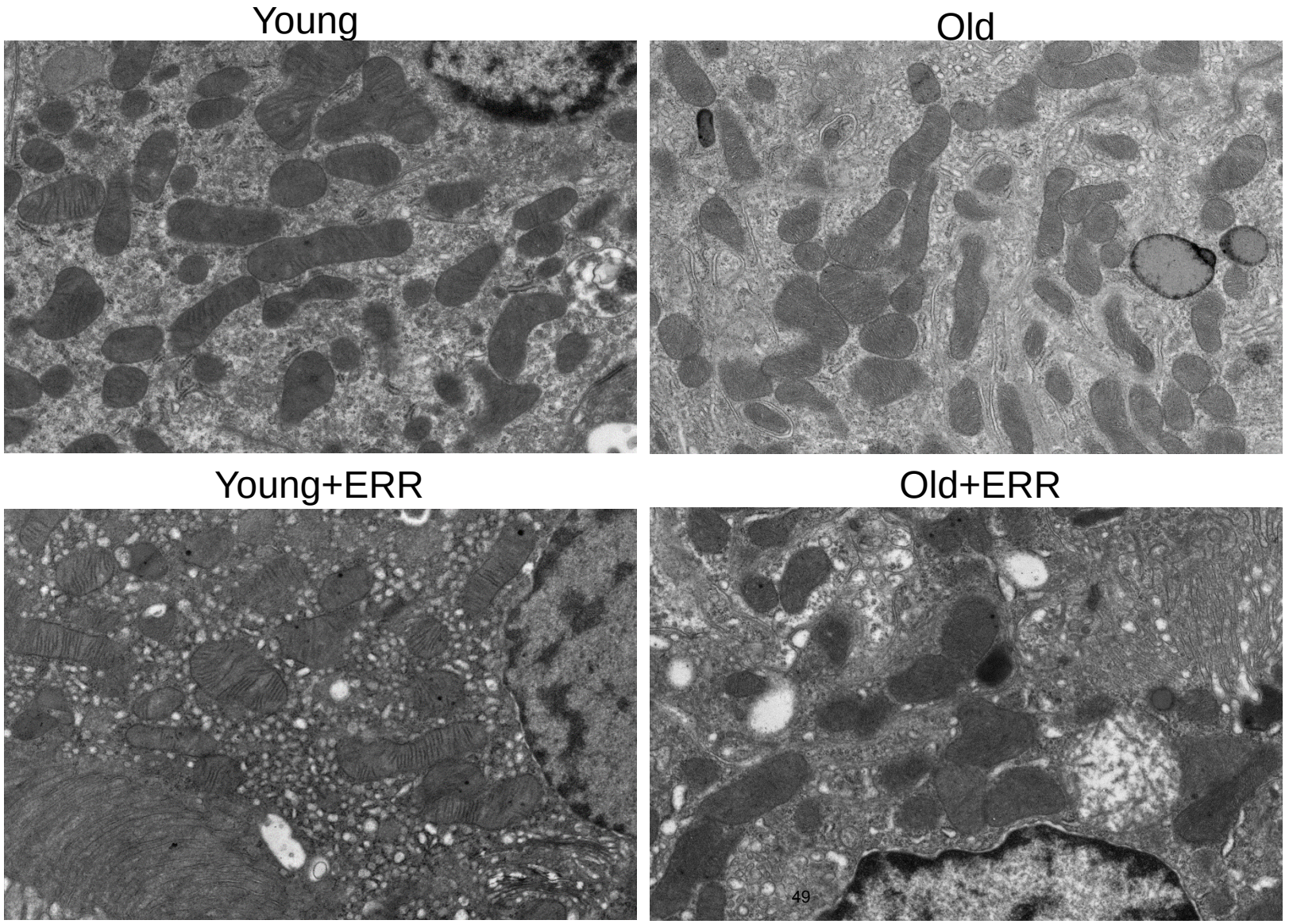
Young
Old
Young+ERR
Old+ERR

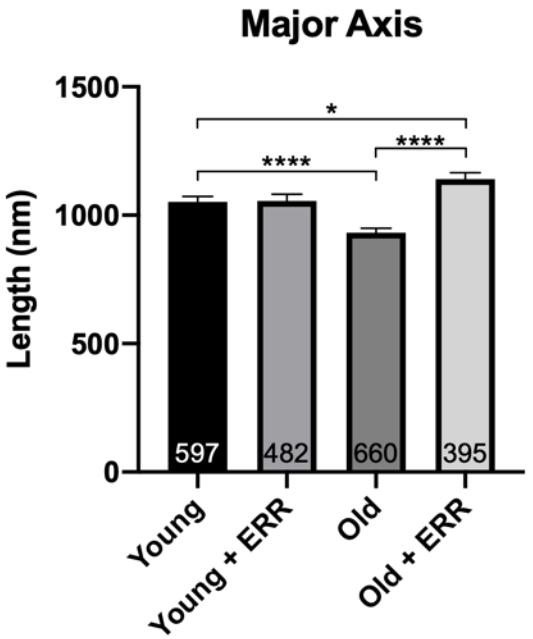
Major Axis
Length (nm)
1500
1000
500
0
*
****
****
597
482
660
395
Young
Young + ERR
Old
Old + ERR

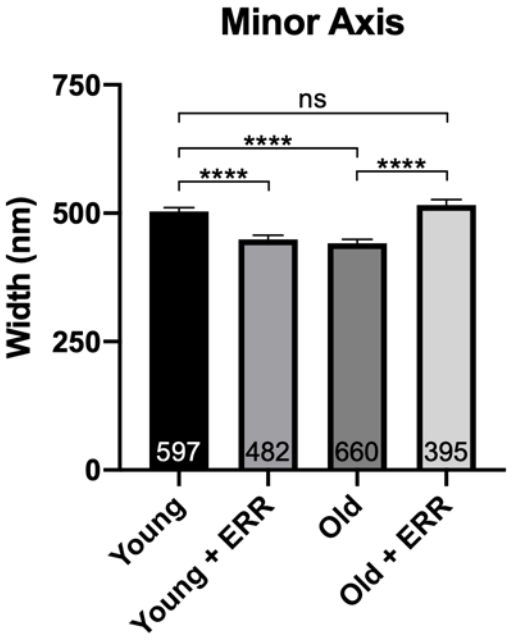
Minor Axis
Width (nm)
750
500
250
0
ns
****
****
597
482
660
395
Young
Young + ERR
Old
Old + ERR

Figure 9

B

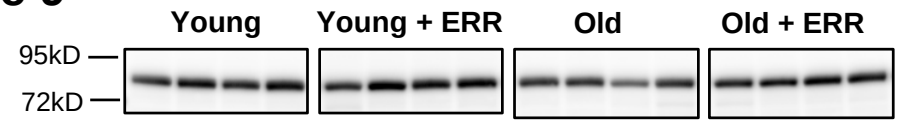
Young
Young + ERR
Old
Old + ERR
95kD
72kD

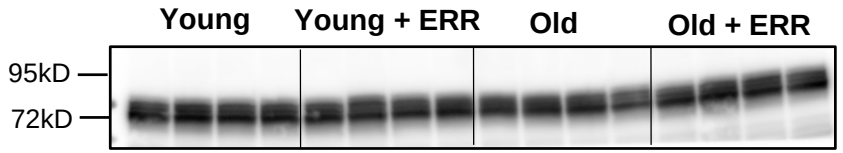
Young
Young + ERR
Old
Old + ERR
95kD
72kD

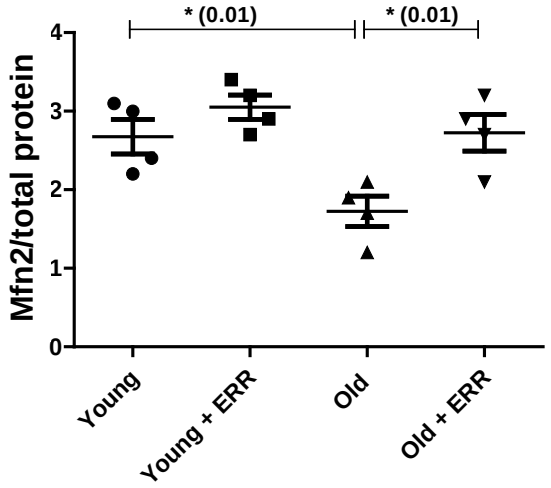
* (0.01)
* (0.01)
Mfn2/total protein
0
1
2
3
4
Young
Young + ERR
Old
Old + ERR

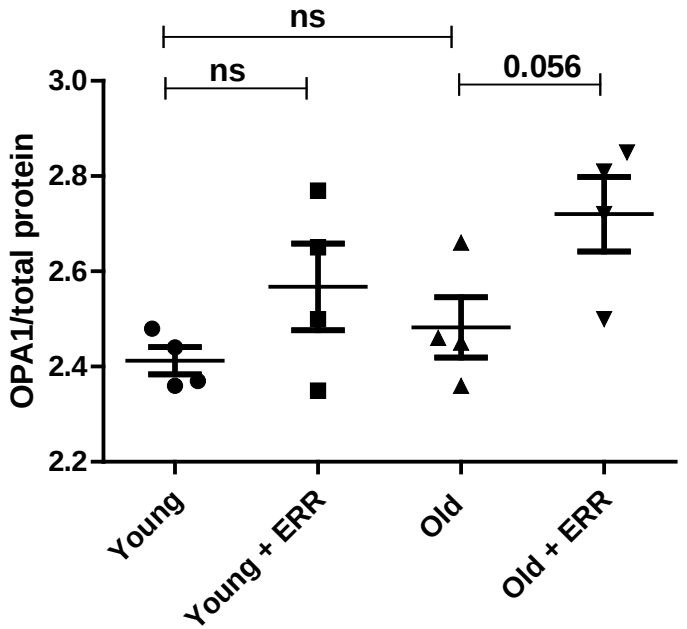
ns
ns
0.056
OPA1/total protein
2.2
2.4
2.6
2.8
3.0
Young
Young + ERR
Old
Old + ERR

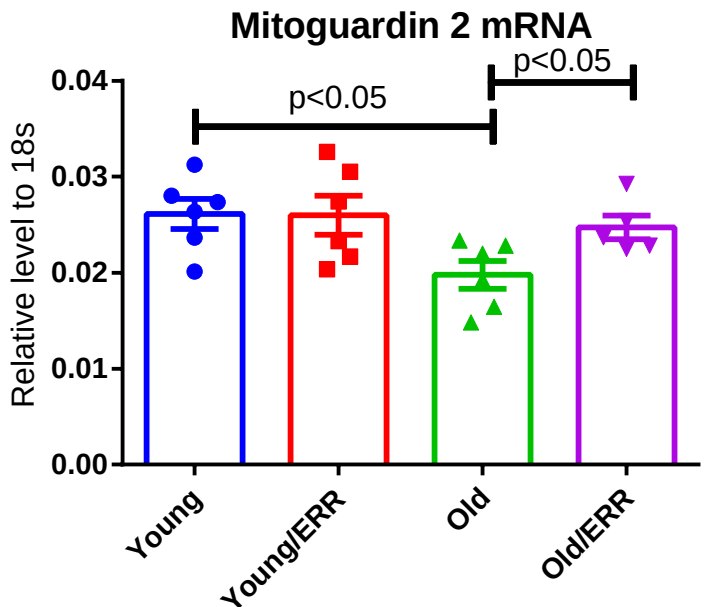
Mitoguardin 2 mRNA
p<0.05
p<0.05
Relative level to 18s
0.00
0.01
0.02
0.03
0.04
Young
Young/ERR
Old
Old/ERR

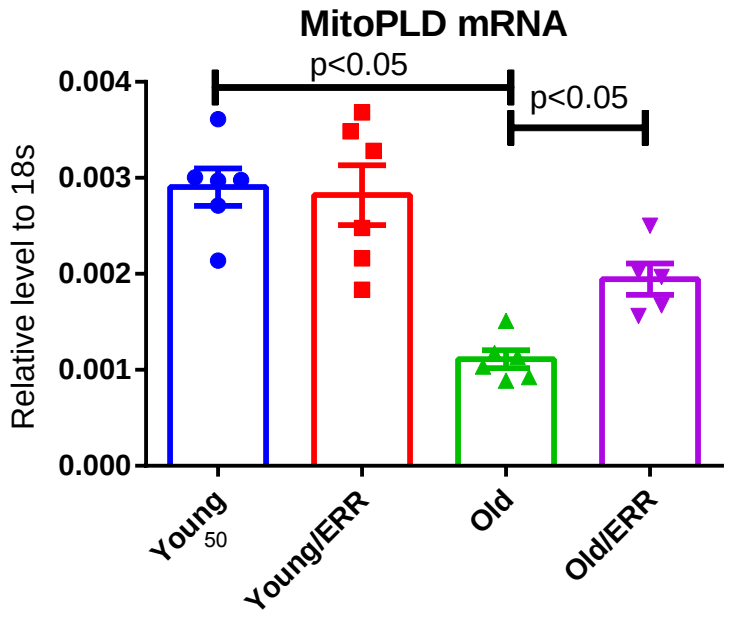
MitoPLD mRNA
p<0.05
p<0.05
Relative level to 18s
0.000
0.001
0.002
0.003
0.004
Young
Young/ERR
Old
Old/ERR

Figure 9

C

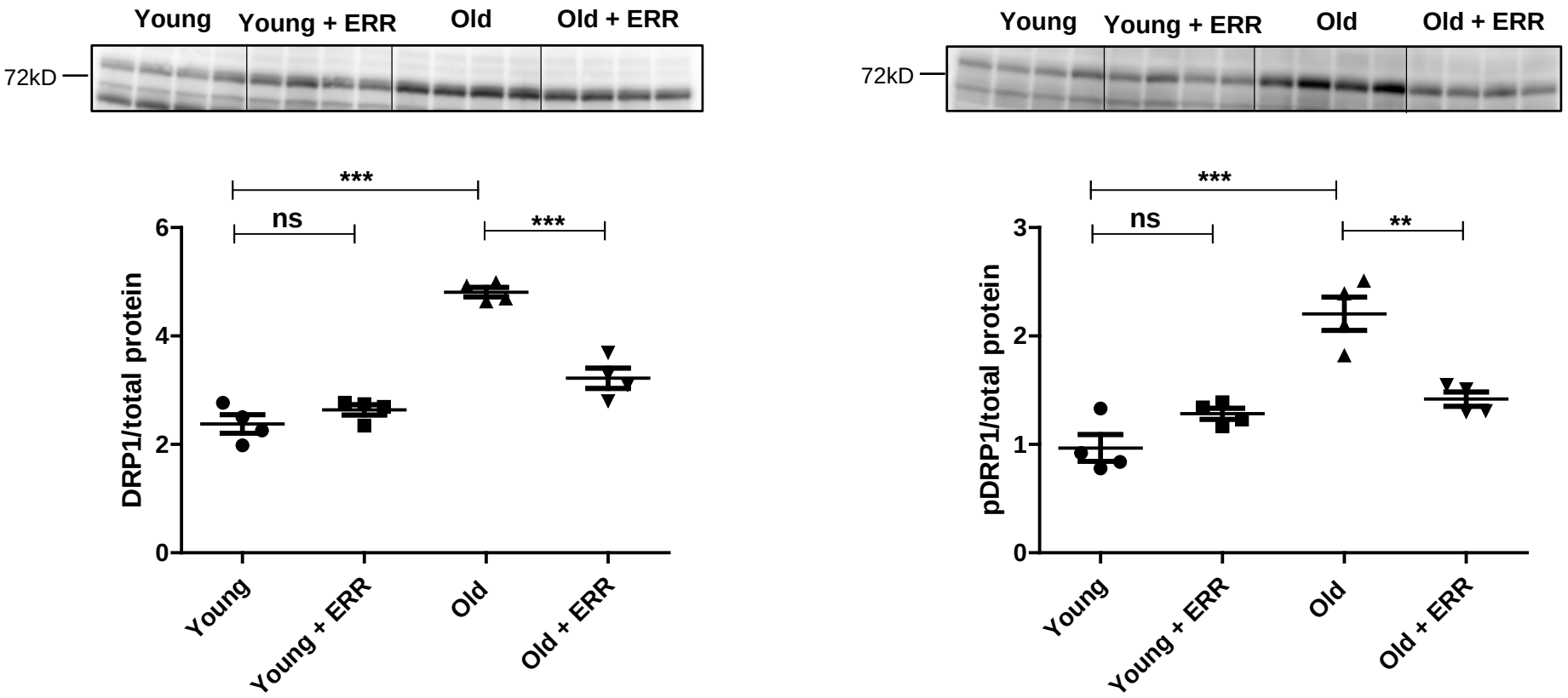
Young
Young + ERR
Old
Old + ERR
72kD
***
ns
***
DRP1/total protein
6
4
2
0
Young
Young + ERR
Old
Old + ERR
Young
Young + ERR
Old
Old + ERR
72kD
***
ns
**
pDRP1/total protein
3
2
1
0
Young
Young + ERR
Old
Old + ERR

Figure 10

A

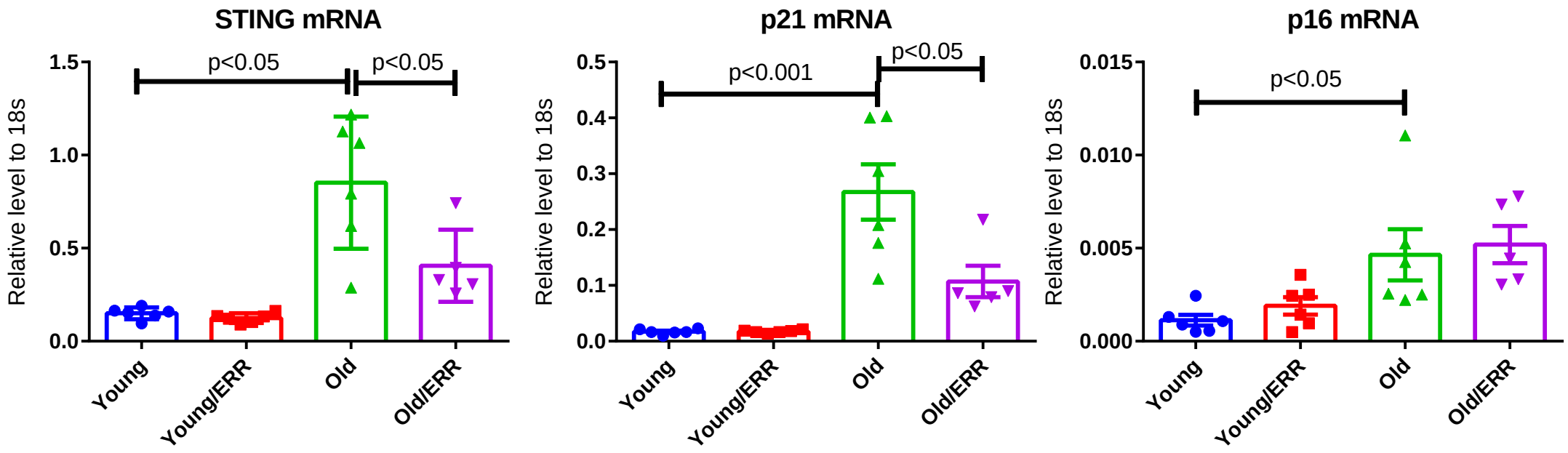
STING mRNA
Relative level to 18s
1.5
1.0
0.5
0.0
p<0.05
p<0.05
Young
Young/ERR
Old
Old/ERR
p21 mRNA
Relative level to 18s
0.5
0.4
0.3
0.2
0.1
0.0
p<0.001
p<0.05
Young
Young/ERR
Old
Old/ERR
p16 mRNA
Relative level to 18s
0.015
0.010
0.005
0.000
p<0.05
Young
Young/ERR
Old
Old/ERR

Figure 10

B

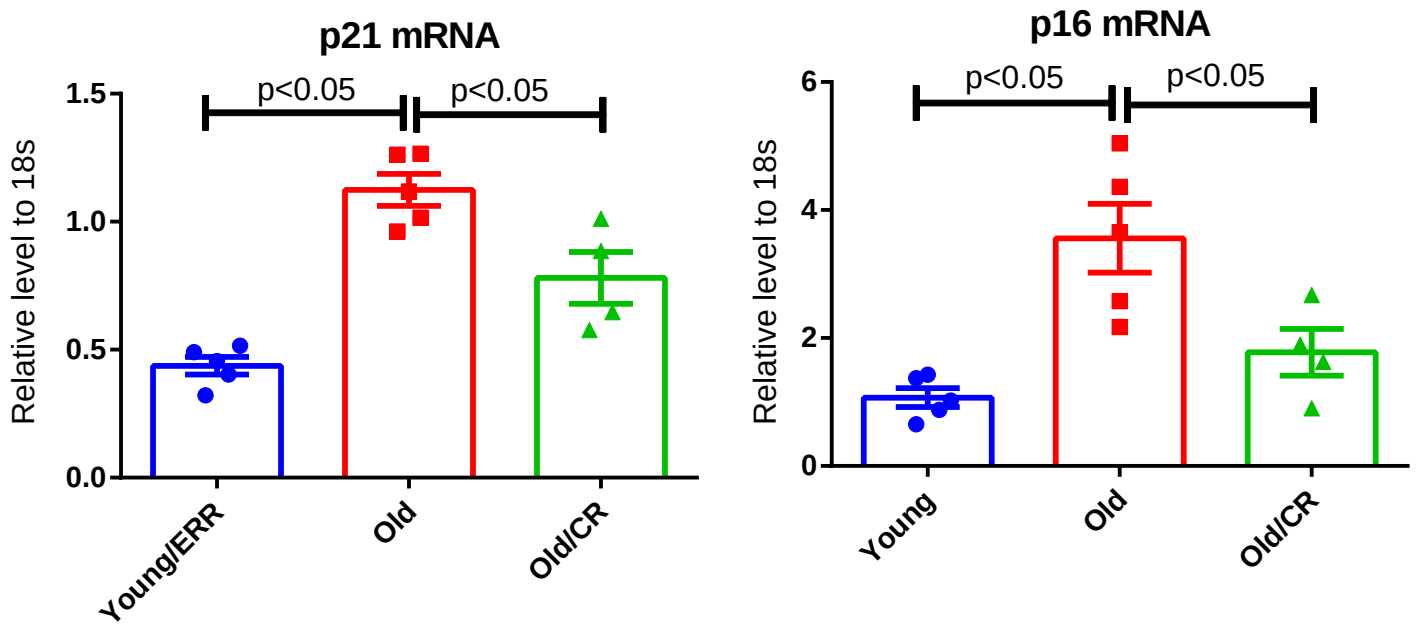
p21 mRNA
p<0.05
p<0.05
Relative level to 18s
1.5
1.0
0.5
0.0
Young/ERR
Old
Old/CR
p16 mRNA
p<0.05
p<0.05
Relative level to 18s
6
4
2
0
Young
Old
Old/CR

Figure 10

C

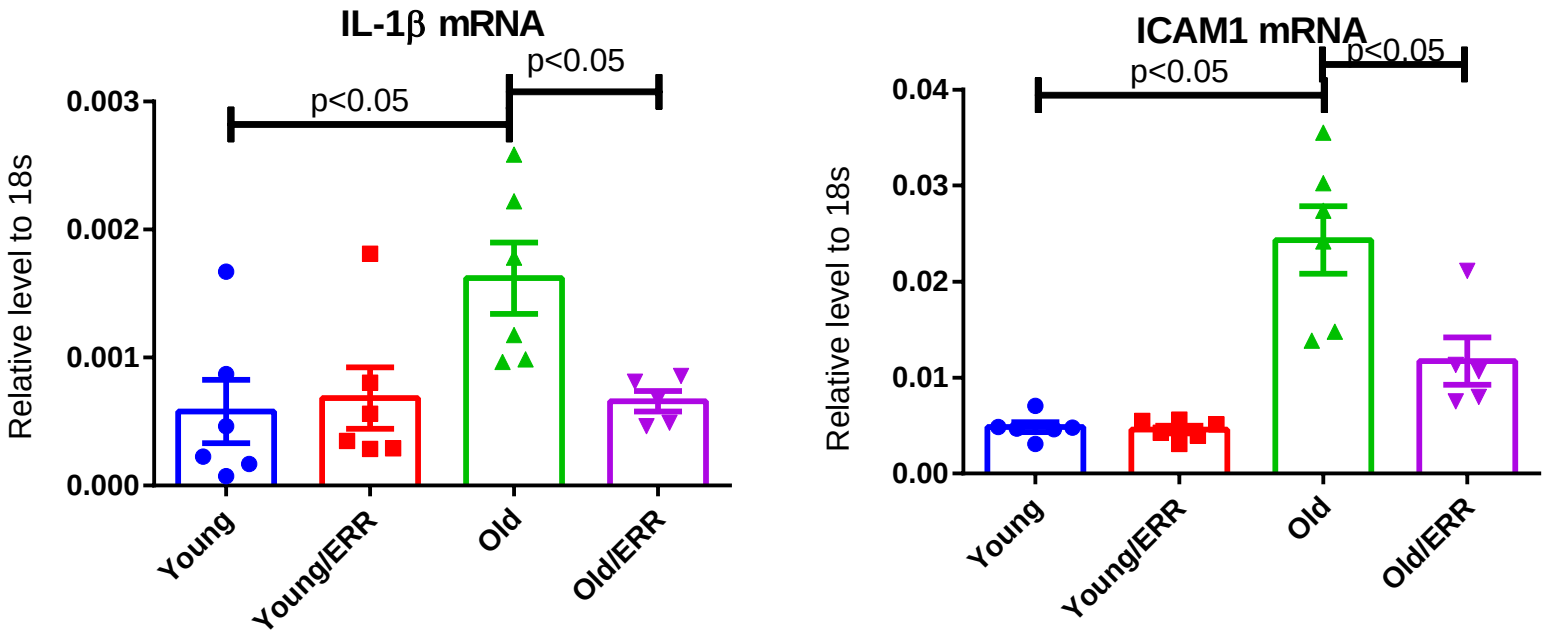
IL-1β mRNA
p<0.05
p<0.05
Relative level to 18s
0.003
0.002
0.001
0.000
Young
Young/ERR
Old
Old/ERR
ICAM1 mRNA
p<0.05
p<0.05
Relative level to 18s
0.04
0.03
0.02
0.01
0.00
Young
Young/ERR
Old
Old/ERR

Figure 10

D

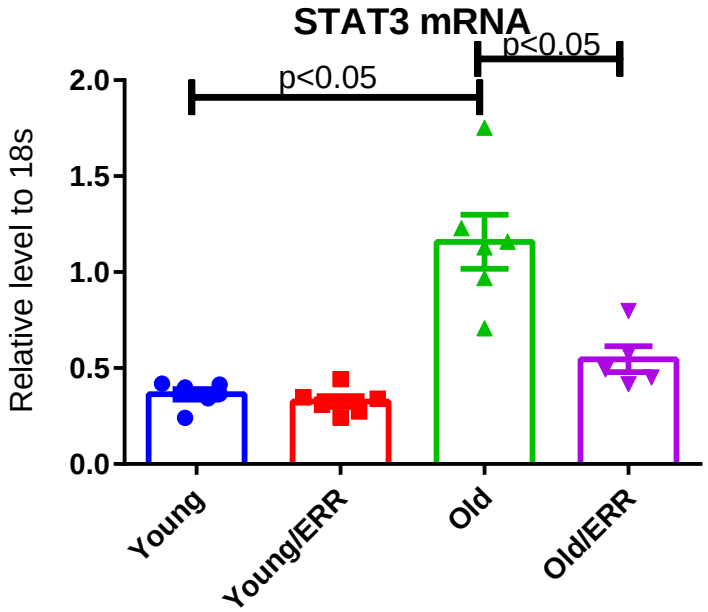
STAT3 mRNA
p<0.05
p<0.05
Relative level to 18s
2.0
1.5
1.0
0.5
0.0
Young
Young/ERR
Old
Old/ERR

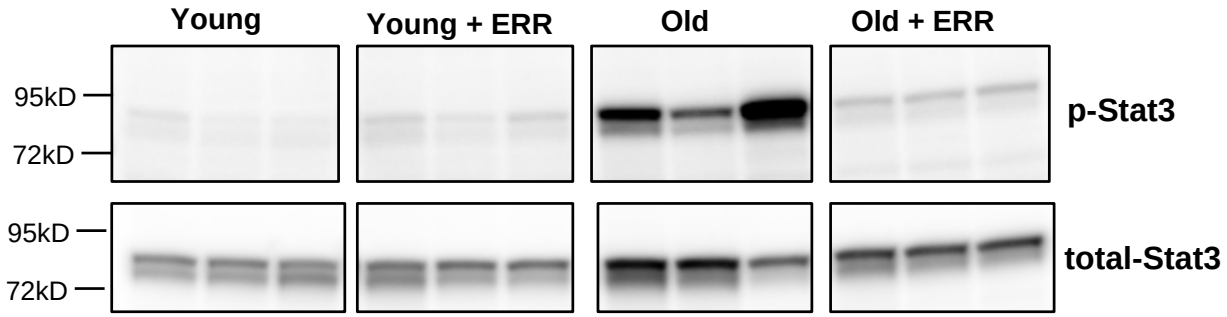
Young
Young + ERR
Old
Old + ERR
95kD
72kD
95kD
72kD
p-Stat3
total-Stat3

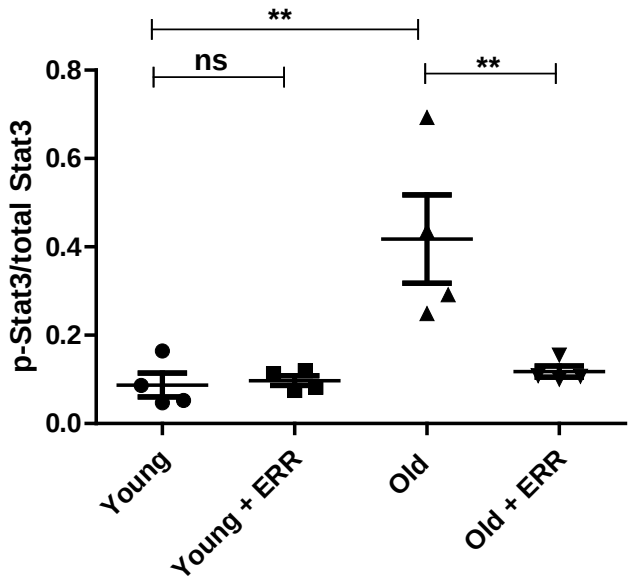
**
ns
**
p-Stat3/total Stat3
0.8
0.6
0.4
0.2
0.0
Young
Young + ERR
Old
Old + ERR

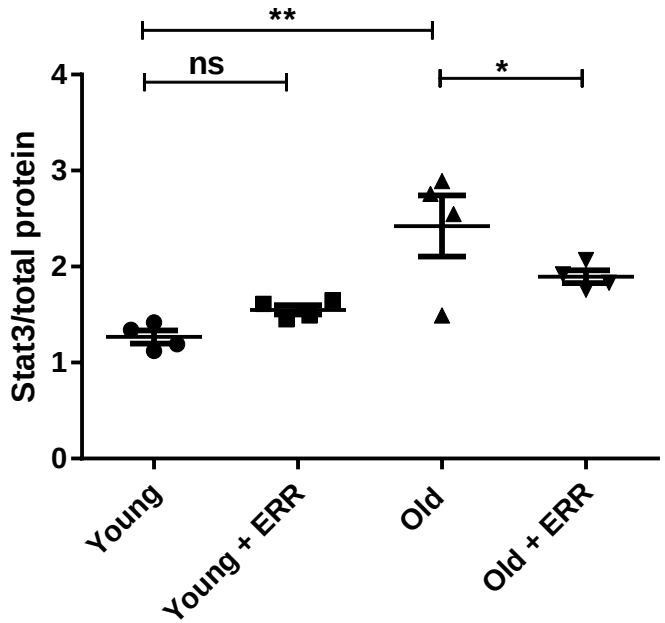
**
ns
*
Stat3/total protein
4
3
2
1
0
Young
Young + ERR
Old
Old + ERR